Title
The 20 Vertex Model and Related Domino Tilings

Author
Huang, Frederick

Publication Date
2023

Peer reviewed|Thesis/dissertation

The 20 Vertex Model and Related Domino Tilings

by

Frederick Huang

A dissertation submitted in partial satisfaction of the

requirements for the degree of

Doctor of Philosophy

in

Mathematics

in the

Graduate Division

of the

University of California, Berkeley

Committee in charge:

Professor Sylvie Corteel, Chair
Professor Mark Haiman
Professor David Nadler

Spring 2023

The 20 Vertex Model and Related Domino Tilings

Abstract

The 20 Vertex Model and Related Domino Tilings

by

Frederick Huang

Doctor of Philosophy in Mathematics

University of California, Berkeley

Professor Sylvie Corteel, Chair

A configuration of the twenty vertex model is an orientation of each edge in a triangular lattice such that at each vertex the number of incoming and outgoing edges is equal. This is similar to the six vertex model, which takes place on a square lattice, that has long been of interest to combinatorialists for its connections to alternating sign matrices. Recently Di Francesco and Guitter uncovered interesting combinatorics for the twenty vertex model which previously was primarily studied by physicists. Di Francesco was also able to relate configurations of the twenty vertex model to domino tilings of a so-called Aztec triangle, and conjectured a product formula for enumerating these configurations. We examine the enumeration of these objects including several combinatorial bijections of the twenty vertex model. In particular we establish a relation from the aforementioned domino tilings to sequences of partitions, and then introduce a generalized Aztec triangle for which we obtain a generalization to Di Francesco's conjecture.

Contents

List of Figures

Acknowledgments

I would like to extend my sincere thanks to my adviser, Sylvie Corteel, for her invaluable advice, encouragement, and patience throughout my time at Berkeley. Without her guidance my degree would not have been possible.

Many thanks also to my parents, who fostered in me my curiosity and interest in mathematics. Both of them, along with my brother and my girlfriend have provided me constant support – emotional and otherwise. I am truly lucky to have them all in my life.

And finally thanks to my friends, both new and old, who made my experience at Berkeley that much more enjoyable. They are what I miss most from the Bay Area.

Chapter 1

Introduction

Recently Di Francesco and Guitter [9] uncovered interesting combinatorics regarding the twenty vertex (20V) model, which previously was of interest to physicists [1] [13]. The 20V model considers all orientations on the edges on some finite portion of a triangular lattice, shown in Figure 1.1, such that at each vertex the number of ingoing edges is equal to the number of outgoing edges. Since each such vertex is adjacent to six edges in the triangular lattice, of which three must be ingoing and three must be outgoing, we see that there are exactly twenty possible configurations of edges at a vertex – hence the name twenty vertex model. The 20V model is analogous to the six vertex (6V) model [4], which uses a square lattice (with six possible configurations of edges at a vertex). This 6V model is famously used to in a proof of the alternating sign matrix (ASM) theorem [17], ie. that the number of $n \times n$ ASMs is given by $\prod_{i=0}^{n-1} \frac{(3i+1)!}{(n+i)!}$ [19, A005130]. ASMs have long been of interest to combinatorialists, with the first proof of this theorem regarding their enumeration in [23].

In [9] Di Francesco and Guitter show that the number of configurations of the 20V model on a square domain (with particular boundary conditions) can be counted by (a weighted enumeration of) configurations of the 6V model on an analogous domain (in fact, the ones from the ASM theorem). Chapter 2 explores several bijections for the 20V model on square domains, including its poset structure, pairs of symplectic tableaux, and alternating phase matrices, which Di Francesco and Guitter define in [9].

By considering 20V models on a larger domain named an Aztec triangle, an example of which is in Figure 1.2, Di Francesco [8] later also conjectures that 20V models on these domains are counted by $2^{n(n-1)/2} \prod_{i=0}^{n-1} \frac{(4i+2)!}{(n+2i+1)!}$ [19, A341275] which strikingly resembles the formula from the ASM theorem. In the same paper [8], Di Francesco establishes that configurations of the 20V model on this expanded domain are equal in number to domino tilings of a particular domain, one such example pictured in Figure 1.2. Though notably there is no combinatorial bijection between these two sets of equal size.

In Chapter 3 we interpret domino tilings of these domains from [8] as sequences of partition $\lambda^{(0)} = (0, \ldots, 0), \ldots, \lambda^{(2n-1)} = (n, n-1, \ldots, 1)$ subject to certain conditions, like those seen in [2]. More generally we are able to construct domains, which we call generalized

Aztec triangles, for sequences where the final partition is not $(n, n-1, \ldots, 1)$ as well as for sequences of greater length. From here we provide a number of ways to enumerate the domino tilings for our domains and provide a generalization to Di Francesco's formula for when the final partition is $(k, k-1, \ldots, 1, 0^{n-k})$, thereby proving Di Francesco's conjecture for when $n = k$. In particular when the final partition is $\lambda^{(\ell-1)} = (k, k-1, \ldots, 1, 0^{n-k})$ with either $\ell = 2n$ or $\ell = 2n+1$, domino tilings of the corresponding generalized Aztec triangle are enumerated by

$$\prod_{i\geq 0}\left(\prod_{s=-2k+4i+1}^{-k+2i}(\ell+s)\prod_{s=k-2i}^{2k-4i-2}(\ell+s)\right)\Bigg/\prod_{i=1}^{k-1}(2i+1)^{k-i}$$

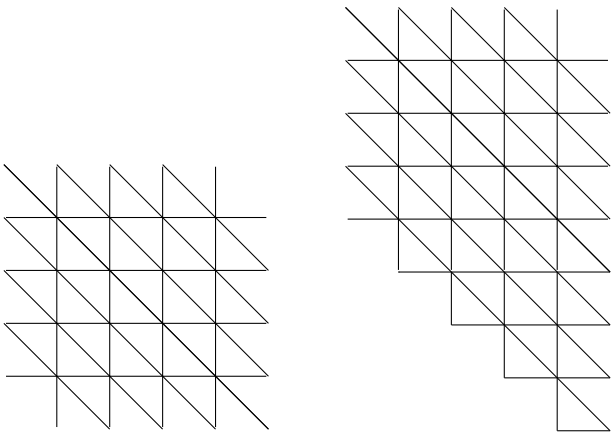

Figure 1.1: On the left is pictured a domain of the 20V model considered in [9], in which configurations of various boundary conditions are counted. On the right is an example of another domain of interest, which is considered in [8].

1.1 Background

Let us begin with several preliminary definitions.

Definition 1.1.1. A *partition* $\mu = (\mu_1, \ldots, \mu_n)$ is a sequence of non-negative integers such that $\mu_1 \geq \mu_2 \geq \cdots \geq \mu_n$. We call $\mu_1, \ldots, \mu_n$ the *parts* of the partition μ, and n the *length* of the partition μ. Any partition of length n can also be considered a partition of length m for any $m \geq n$ (or even m infinite) by appending 0's at the end of the partition..

We also define the *conjugate* partition of μ to be the partition μ' of length μ_1 such that $\mu'_i = \#\{\mu_j \mid \mu_j \geq i\}$.

A *Young diagram* is a collection of boxes arranged in rows such that the rows are left justified and non-decreasing from bottom to top. We can visualize a partition μ as a Young diagram with rows of lengths equal to the parts of μ, as illustrated in Figure 1.3.

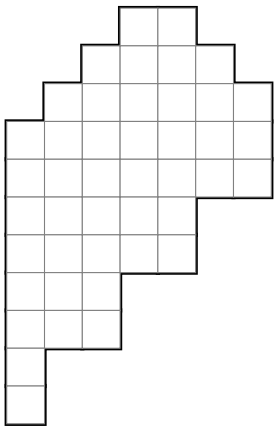

Figure 1.2: An example of an Aztec triangle considered by Di Francesco in [8] whose domino tilings are equal in number to 20V configurations on the domain on the right in Figure 1.1.

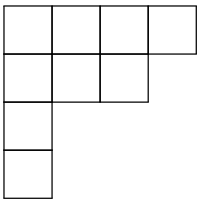

Figure 1.3: The Young diagram corresponding to the partition $\mu = (4, 2, 1, 1)$.

Definition 1.1.2. For partitions λ, μ of equal length such that $\lambda_i \geq \mu_i$ for all i, we can define the *skew diagram* λ/μ to be the boxes in the Young diagram of λ that are not in the Young diagram of μ. A skew diagram λ/μ is called a *horizontal strip* if its Young diagram contains at most one box in each column. Similarly, it is called a *vertical strip* if λ'/μ' is a horizontal strip, or equivalently if its Young diagram contains at most one box in each row.

In Figure 1.4, we illustrate a few skew diagrams, one of which is a horizontal strip and another a vertical strip.

Definition 1.1.3. A *standard Young tableau* is a filling of the boxes of the Young diagram corresponding to μ with entries $1, 2, 3, \ldots$ such that its rows and columns are strictly increasing.

Definition 1.1.4. A *semistandard Young tableau* is a filling of the boxes of the Young diagram corresponding to μ with entries $1, 2, 3, \ldots$ such that its rows are weakly increasing and columns are strictly increasing.

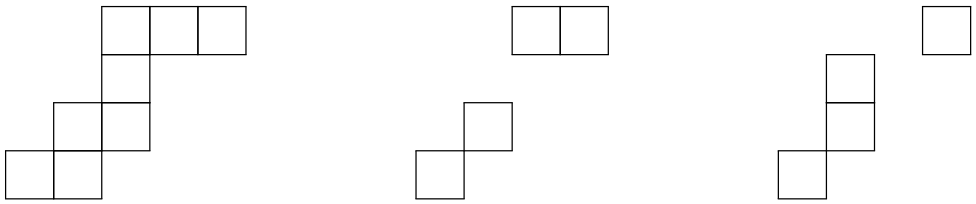

Figure 1.4: Three skew diagrams λ/μ where $\lambda = (5, 3, 3, 2)$. On the left we have $\mu = (2, 2, 1, 0)$. In the center, we have $\mu = (3, 3, 2, 1)$ resulting in a horizontal strip. On the right we have $\mu = (4, 2, 2, 1)$ resulting in a vertical strip.

Definition 1.1.5 ([15, 14, 12])**.** A *semistandard symplectic tableau* of shape μ is a filling of the boxes of the Young diagram corresponding to μ with entries $1 < \overline{1} < 2 < \overline{2} < \cdots$ such that

(1) rows are weakly increasing and columns are strictly increasing.

(2) i and $\bar{\imath}$ do not appear below the ith row.

The first condition is referred to as the semistandard condition, and the second condition is the symplectic condition. Note that we can equivalently state the semi-standard condition of weakly increasing rows and strictly increasing columns as:

(i) rows and columns are weakly increasing.

(ii) for all i, the entries i or $\bar{\imath}$ form horizontal strips.

Definition 1.1.6. A *super symplectic tableau* of shape μ is a filling of boxes of the Young diagram corresponding to μ with entries $1 < \overline{1} < 2 < \overline{2} < \cdots$ such that

(1) rows and columns are weakly increasing

(2) for all i, the entries i form horizontal strips (i.e. there is at most one i in each column).

(3) for all i, the entries $\bar{\imath}$ form vertical strips (ie. there is at most one $\bar{\imath}$ in each row).

The rows of our super symplectic tableaux are overpartitions [7] and, without the symplectic conditions, our tableaux would be super semistandard tableaux [16]. Figure 1.5 provides an examples of our various tableaux.

Vertex Models

Let us now define a number of vertex models, also known as ice models. We start with the most well known vertex model: the six vertex model.

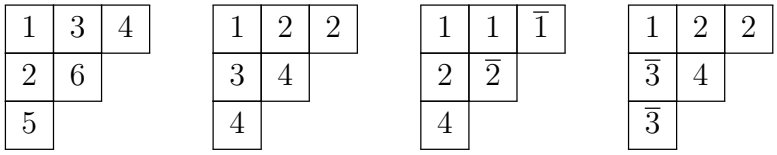

Figure 1.5: In order from left to right: a standard Young tableau, a semistandard Young tableau, a symplectic tableau, and a super symplectic tableau of shape $(3, 2, 1)$.

Definition 1.1.7. Consider the square lattice on the integer points of $[0, n-1]^2$, pictured in Figure 1.6, so that each of these vertices are adjacent to four edges. A configuration of the *6 vertex (6V) model* on this finite domain is an assignment of a direction to each of these edges such that at each vertex the number of incoming and outgoing edges are equal.

We will consider 6V models with a fixed boundary condition, where the horizontal edges on the west and east boundaries are oriented towards the domain and the vertical edges on the north and south boundaries are oriented away from the domain. We use $Z^{6V}(n)$ to denote the set of all such configurations.

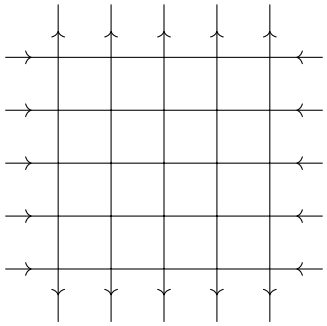

Figure 1.6: The square lattice of the 6V model with our boundary condition.

The 6V model was originally used in statistical mechanics to model ice, in which each oxygen atom is connected by a bond to four other oxygen atoms, via a hydrogen atom. Moreover, exactly two of these four hydrogen atoms are closer to the oxygen atom so that we have an H_2O molecule. In this way, the vertices of our square lattice represent oxygen atoms and the orientation of each edge represents which hydrogen atoms are closest to each oxygen atom.

From Definition 1.1.7 we see that each vertex must have two incoming and two outgoing edges. So there are $\binom{4}{2} = 6$ configurations at each vertex seen in Figure 1.7, hence the name 6 vertex model. We can also interpret a 6V model configuration of $Z^{6V}(n)$ as a collection n

osculating paths by assigning a segment of a path to horizontal edges oriented to the right and vertical edges oriented to down. Indeed we see that with our boundary condition we then must have n paths beginning on the west boundary and ending on the south boundary. See Figure 1.8 for a sample 6V model configuration and its associated osculating paths.

Here we use osculating to mean that our paths are non-intersecting except at some finite number of vertices. In the case of the 6V model, there are vertices where one path comes from the west and turns south, and another comes from the north and turns east. See the first vertex in Figure 1.7.

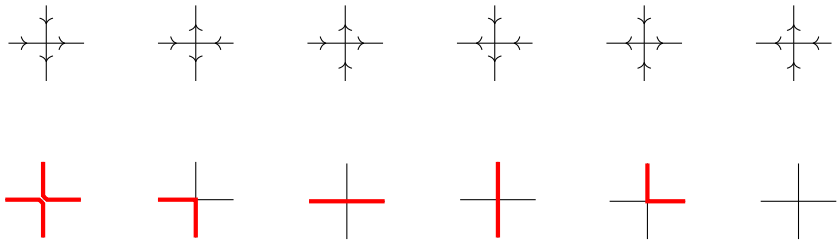

Figure 1.7: The six possible configurations at any vertex of the 6V model and the corresponding paths.

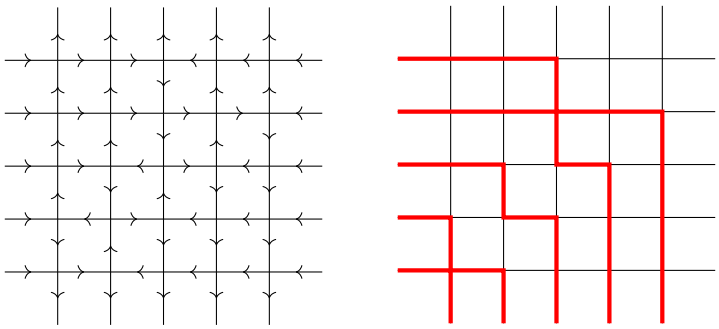

Figure 1.8: A configuration of the 6V model, and the corresponding osculating paths.

Though it had its beginnings in physics, the 6V model has now long been of interest to combinatorialists for its connections to alternating sign matrices.

Definition 1.1.8. An *alternating sign matrix* (ASM) of size n is an $n \times n$ matrix with entries $-1, 0, 1$ such that

- the sum of each row and column is 1
- the nonzero entries in each row and column alternate in sign

Specifically, configurations of the 6V model on $n \times n$ vertices are in bijection with alternating sign matrices of size n [17]. For each vertex in the configuration of the 6V model, we set the corresponding entry in the $n \times n$ ASM to $-1, 0, 1$ according to Figure 1.9 to 1 and -1, for example as shown in Figure 1.10. Moreover, we know from a celebrated theorem [17] [23] about ASMs that the number of ASMs of size n is given by

$$\prod_{i=0}^{n-1} \frac{(3i+1)!}{(n+i)!}$$

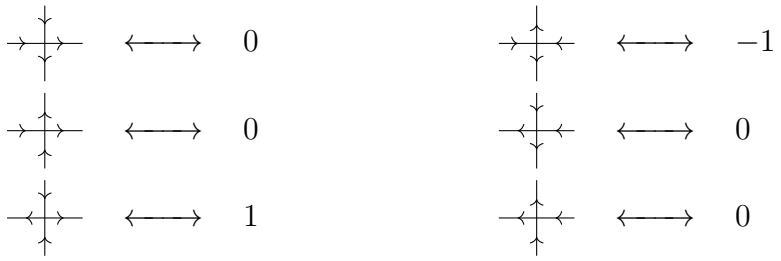

Figure 1.9: Bijection from the 6V model to ASMs.

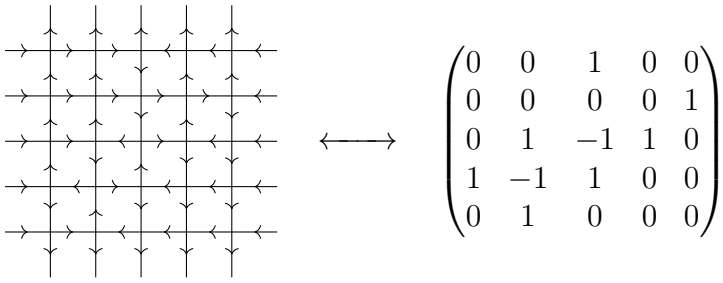

$$\begin{pmatrix} 0 & 0 & 1 & 0 & 0 \\ 0 & 0 & 0 & 0 & 1 \\ 0 & 1 & -1 & 1 & 0 \\ 1 & -1 & 1 & 0 & 0 \\ 0 & 1 & 0 & 0 & 0 \end{pmatrix}$$

Figure 1.10: A configuration of the 6V model on 5×5 vertices, and the corresponding alternating sign matrix of size 5.

Definition 1.1.9. Now consider the triangular lattice on the integer points of $[0, n-1]^2$, pictured in Figure 1.11, so that each of these vertices are adjacent to four edges. A configuration of the *20 vertex (20V) model* on this finite domain is an assignment of a direction to each of these edges such that at each vertex the number of incoming and outgoing edges are equal.

Again we will consider 20V models with a fixed boundary condition, where the horizontal edges on the west and east boundaries are oriented towards the domain and the vertical edges on the north and south boundaries are oriented away from the domain. Moreover the diagonal edges on the main diagonal as well as any diagonals to the southwest are oriented down and to the right, whereas diagonal edges to the northeast of the main diagonal are oriented up and to the left. We also use $Z^{20V}(n)$ to denote the set of all such configurations.

Of course, this is just one of many possible boundary conditions we could take. In [9] there are three boundary conditions which are considered. The one we have in the definition above is called DWBC1, which is also equivalent to the second boundary condition, DWBC2, in said paper. For the third boundary condition of [9], DWBC3, we will consider a different domain.

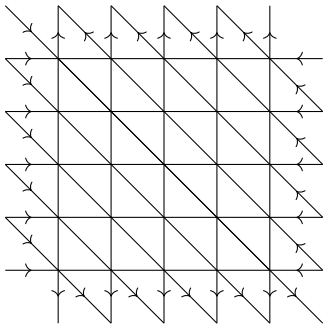

Figure 1.11: The triangular lattice of the 20V model with our boundary condition.

Similar to the 6V model, we see that for the 20V model at each vertex there are $\binom{6}{3} = 20$ possible configurations. We can also interpret configurations of the 20V model as a collection of osculating paths, where we additionally assign segments of paths to diagonal edges oriented down and to the right. In this way we have $2n$ osculating paths for any configuration of $Z^{20V}(n)$, beginning on the west boundary and ending on the south boundary. See Figure 1.13 for a sample 20V model configuration and its associated osculating paths.

For both the 6V and 20V model, we will interchangeably consider them as orientations of edges and osculating paths. Moreover when we consider them as osculating paths, we will refer to the outermost path as the one furthest to the top right.

In [9] Di Francesco and Guitter show the following theorem.

Theorem 1.1.10. *$|Z^{20V}(n)|$ is equal to a weighted enumeration of $Z^{6V}(n)$ where the weight of each configuration of $Z^{6V}(n)$ is determined by the product of the weights of its vertices, and the vertices in Figure 1.14 receive weight $\sqrt{2}$ while the other four types of vertices have weight 1.*

This is proved by using the Yang-Baxter equations to move the move the diagonal edges edges of our 20V model configuration outside the square, thus "unravelling" our 20V model

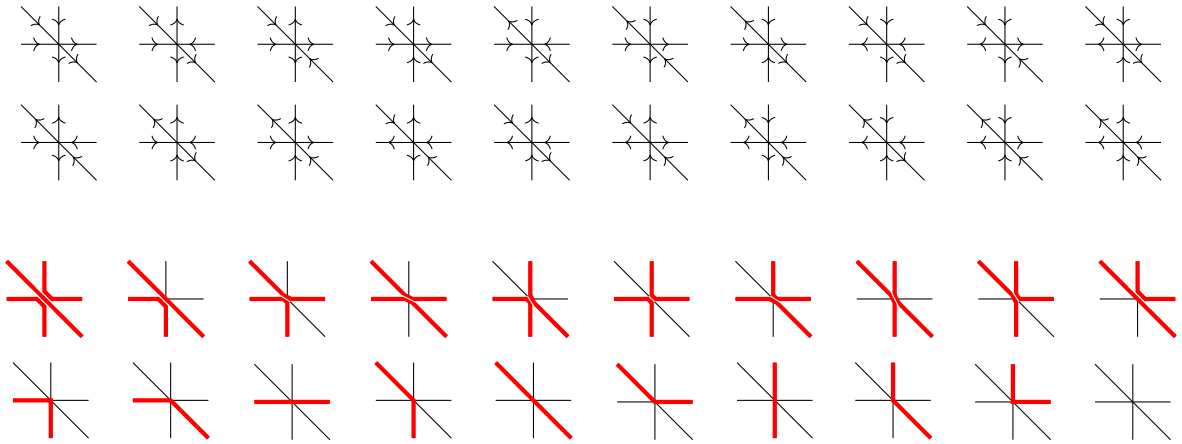

Figure 1.12: The twenty possible configurations at any vertex of the 20V model and the corresponding paths.

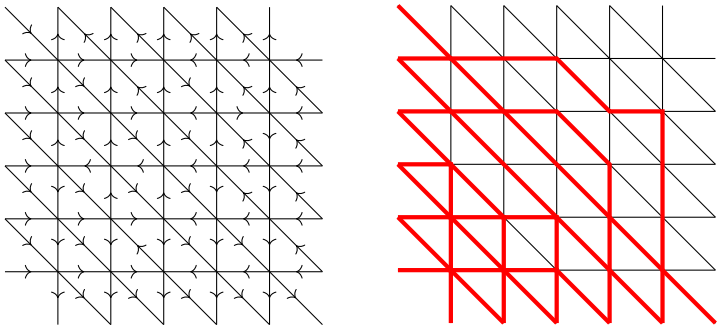

Figure 1.13: A configuration of the 20V model, and its corresponding osculating paths.

configuration into a 6V model configuration (or several configurations – see [1], Section 3 of [9]).

Figure 1.14: The vertices of the 6V model with weight $\sqrt{2}$.

Let us also introduce another collection of configurations of the 20V model which will be of relevance in Chapter 3.

Definition 1.1.11. The trapezoidal domain $\mathcal{T}_n$ is the region bounded by

(i) $0 \leq x \leq n-1$

(ii) $y \leq n-1$

(iii) $x+y \geq 0$

We will consider 20V model configurations on $\mathcal{T}_n$ with the boundary condition that

- horizontal edges are oriented towards the domain.
- vertical edges are oriented away from the domain.
- diagonal edges along the west and north boundary are oriented away from the domain, and diagonal edges along the east boundary are oriented towards the domain.

The domain $\mathcal{T}_5$ along with its boundary condition is pictured in Figure 1.15.

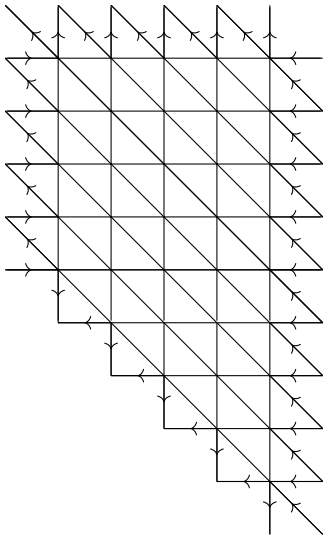

Figure 1.15: The domain $\mathcal{T}_5$ with its boundary condition for the 20V model.

Chapter 2

Combinatorial Bijections

In this section we will identify a few combinatorial bijections for the 20V model on a square domain with the boundary condition DWBC1 from Definition 1.1.9. In doing so, we draw inspiration from analogous bijections for the 6V model, beginning with examining its poset structure as done in [22] and concluding with an analog to the 6V model and ASM bijection.

2.1 The Poset Perspective

Definition 2.1.1. A *poset* $(P, \leq)$ is a set of elements P and a relation $\leq$ such that we have

1. Reflexivity: for all $a \in P$, $a \leq a$.
2. Antisymmetry: if $a \leq b$ and $b \leq a$ then $a = b$.
3. Transitivity: if $a \leq b$ and $b \leq c$ then $a \leq c$.

We can represent a poset by its *Hasse diagram*, where each element of P is represented by a vertex. Also for $a, b \in P$, we draw a below b if $a \leq b$, and connect them with a line if b *covers* a – that is there does not exist any $c \in P$ with $a \leq c \leq b$.

Figure 2.1 shows the Hasse diagram of the power set on three elements, ie. the set of subsets of a three element set, ordered by inclusion.

Let us make some more definitions for posets which we will use in this section.

Definition 2.1.2. A *lower set* I of a poset $(P, \leq)$ is a subset $I \subseteq P$ such that for all $x \in I$ and $p \in P$, if $p \leq x$ then $p \in I$. For any poset $(P, \leq)$, we use $J(P)$ to denote the set of all lower sets of P. $J(P)$ itself is also a poset, ordered by inclusion.

An *interval* I of a poset $(P, \leq)$ is a subset $I \subseteq P$ such that for all $x, y \in I$ and $p \in P$, if $x \leq p \leq y$ then $p \in I$. For $a, b \in P$ we will denote $[a, b]$ to be the interval consisting of all elements $p \in P$ satisfying $a \leq p \leq b$.

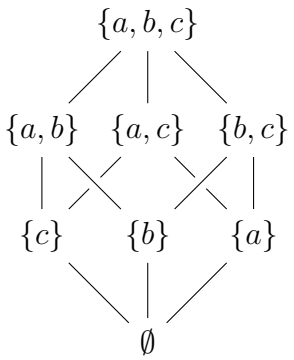

Figure 2.1: The Hasse diagram of the power set on three elements a, b, c ordered by inclusion.

In [22] (whence the title of this section derives) Striker studies the poset structure of ASMs, and hence also the 6V model, of a fixed size n. We will use an equivalent construction to Striker's to realize this poset. First define three vectors

$$\vec{b} = (1, 1, 0), \qquad \vec{y} = (0, 1, 1), \qquad \vec{r} = (0, 2, 0)$$

and consider the points in the set

$$T_n = \{c_1\vec{b} + c_2\vec{y} + c_3\vec{r} \mid c_1, c_2, c_3 \in \mathbb{Z}_{\geq 0},\ c_1 + c_2 + c_3 \leq n - 2\}$$

which are the lattice points of some tetrahedron. Now if we also define the vectors

$$\vec{g} = (1, -1, 0), \qquad \vec{o} = (0, -1, 1)$$

then we have the following proposition (2.5.2 in [22]):

Proposition 2.1.3. *Consider T_n as a poset with the relation that for $x, y \in T_n$ we have $x \leq y$ if $y - x \in \{c_1\vec{b} + c_2\vec{g} + c_3\vec{y} + c_4\vec{o} \mid c_1, c_2, c_3, c_4 \in \mathbb{Z}_{\geq 0}\}$. Then the lower sets $J(T_n)$ are in bijection with $n \times n$ alternating sign matrices.*

We illustrate an example of T_n with its poset structure in Figure 2.2 via its Hasse diagram.

This bijection is provided in [22] and induces a poset structure on the set of $n \times n$ alternating sign matrices. Since $n \times n$ alternating sign matrices are in bijection with 6V model configurations on $n \times n$ vertices, we have the following corollary.

Corollary 2.1.4. *There is a poset structure on $Z^{6V}(n)$ consistent with the poset structure on ASMs of size n.*

Let us describe the poset structure on $Z^{6V}(n)$, the number of 6V model configurations on an $n \times n$ square lattice as defined in Definition 1.1.7. For any two configurations $A, B \in$

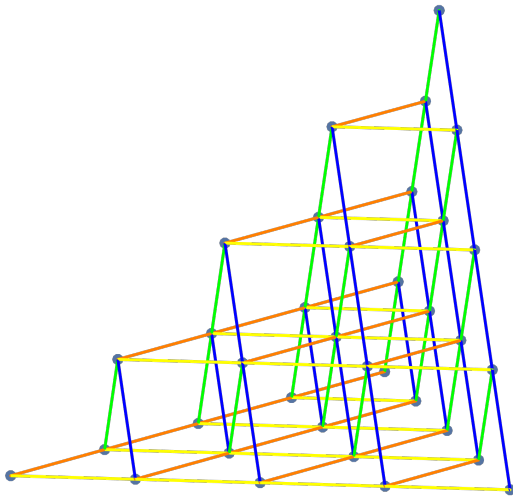

Figure 2.2: The Hasse diagram for the poset T_6. $\vec{b}$ corresponds to the blue edges, $\vec{g}$ the green edges, $\vec{y}$ the yellow edges, and $\vec{o}$ the orange edges.

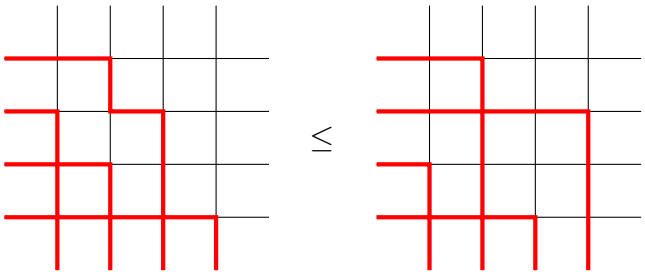

Figure 2.3: An example of the poset structure on 6V model configurations.

$Z^{6V}(n)$, we have $B \leq A$ if each path in B is below and to the left of the corresponding path in A, as shown in Figure 2.3.

It follows that for two configurations $A, B \in Z^{6V}(n)$, we have that A covers B if they are equal except at a group of 2×2 vertices where some path of B takes a downward then eastward step, which becomes an eastward then downward step in A. See Figure 2.4. In this case, we will say that configuration B has been *raised* to the configuration A. Note that in order to perform this raising operation, not only do we need there to be edges for us to raise but we also need that the edges we are raising to are not already occupied by some other

path. Note that then we can restate our poset relation as $B \leq A$ if there exists some (not unique) sequence of raising operations that we apply to B to obtain A.

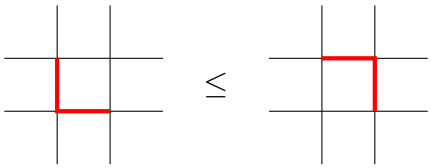

Figure 2.4: The covering relation for the poset structure on 6V model configurations.

We can precisely state the bijection from $J(T_n)$ to $Z^{6V}(n)$. Each point in $a \in T_n$ represents a raising operation as in Figure 2.4 on a specific path. In particular we can uniquely write $a = c_1\vec{b} + c_2\vec{y} + c_3\vec{r}$ where $c_1, c_2, c_3 \in \mathbb{Z}_{\geq 0}$. Then c_2 tells us which path is being raised, and c_1 tells how far up the corner being raised is. Specifically, if the c_2th outermost path starts at $(-1, n-1-c_2)$ then that path is being raised from having a corner at $(c_1+c_3, n-2-c_2-c_3)$ to having one at $(c_1 + c_3 + 1, n - 1 - c_2 - c_3)$.

Then for any $I \in J(T_n)$, the corresponding configuration in $Z^{6V}(n)$ is that which results from performing all its raising operations on the smallest element of $Z^{6V}(n)$, pictured in Figure 2.5.

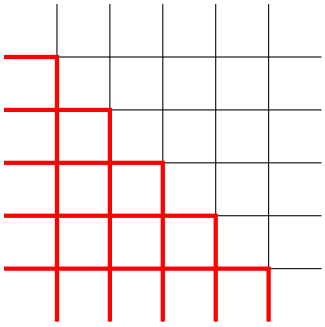

Figure 2.5: The smallest element of $Z^{6V}(5)$.

Our goal now is to construct the poset S_n for which its lower sets $J(S_n)$ are in bijection with $Z^{20V}(n)$: the number of 20V model configurations on a triangular lattice of $n \times n$ vertices, with the boundary condition DWBC1, as defined in Definition 1.1.9. We will use a similar poset structure on $Z^{20V}(n)$ as we do for $Z^{6V}(n)$: for two configurations $A, B \in Z^{20V}(n)$ we have $B \leq A$ if each path in B is below and to the left of the corresponding path in A. Figure 2.6 illustrates an example of such configurations $A, B \in Z^{20V}(3)$.

Similar to the 6V model, we see that for $A, B \in Z^{20V}(n)$ we have A covers B if they are equal except at a group of 2×2 vertices where either

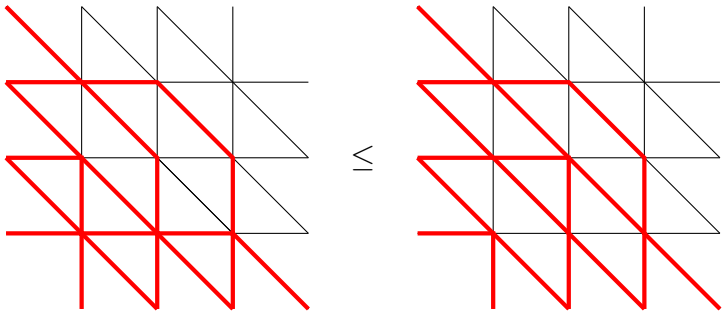

Figure 2.6: An example of the poset structure on 20V model configurations.

- some path of B takes a downward then eastward step, which becomes a diagonal step in A
- or some path of B takes a diagonal step, which becomes an eastward then downward step in A.

See Figure 2.7 for these relations. Again we see that we can restate our poset relation as $B \leq A$ if there exists some sequence of these raising operations that we can apply to B to obtain A.

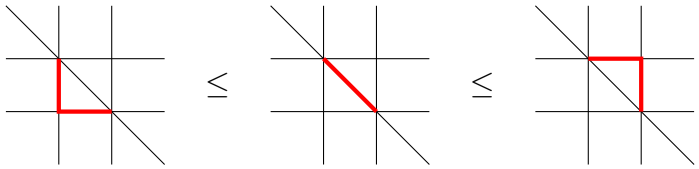

Figure 2.7: The covering relations for the poset structure on 20V model configurations.

Because our previous covering relation in $Z^{6V}(n)$ now goes through an intermediate configuration in $Z^{20V}(n)$, our poset S_n should be obtained by replacing each point in $a \in T_n$ with two points $a, a' \in S^n$ where $a \leq a'$. In addition to our previously defined

$$\vec{b} = (1, 1, 0) \qquad \vec{g} = (1, -1, 0) \qquad \vec{y} = (0, 1, 1) \qquad \vec{o} = (0, -1, 1)$$

define also

$$\vec{l} = (1, 0, 0) \qquad \vec{w} = (0, 0, 1)$$

Then we can exactly construct S_n as follows.

Proposition 2.1.5. *Let S_n be the poset constructed by*

1. *Starting with the points $(0, 2m, 0)$ for $m = 0, \ldots, n-1$*
2. *At each of these points we can add one of $\{\vec{b}, \vec{g}, \vec{w}\}$.*
3. *Whenever we add one of $\{\vec{b}, \vec{g}, \vec{w}\}$ we must then add one of $\{\vec{y}, \vec{o}, \vec{l}\}$ next, and vice versa.*

subject to $x \geq 0$, $z \geq 0$ and either

$$\begin{cases} 3x + 2y + z \leq 4n - 3 \\ 3x - 2y + z \leq 1 \end{cases} \quad \text{or} \quad \begin{cases} x + 2y + 3z \leq 4n - 4 \\ x - 2y + 3z \leq 0 \end{cases}$$

with the relation that for $a, b \in S_n$ we have $b \leq a$ if

$$a - b \in \{c_1\vec{b} + c_2\vec{g} + c_3\vec{w} + c_4\vec{y} + c_5\vec{o} + c_6\vec{l} \mid c_i \in \mathbb{Z}_{\geq 0}\}$$

That is $a - b$ is some conical combination of $\vec{b}, \vec{g}, \vec{w}, \vec{y}, \vec{o}, \vec{l}$. Then there exists a bijection from its lower sets $J(S_n)$ to configurations of the 20V model $Z^{20V}(n)$.

We see that for $a, b \in S_n$ we have that a covers b precisely if

$$a - b \in \{\vec{b}, \vec{g}, \vec{w}, \vec{y}, \vec{o}, \vec{l}\}$$

So as in our tetrahedral poset T_n we can draw the Hasse diagram for S_n using exactly the vectors $\vec{b}, \vec{g}, \vec{w}, \vec{y}, \vec{o}, \vec{l}$. See Figure 2.8.

Proof of Proposition 2.1.5. We can explicitly state the bijection in Proposition 2.1.5 by referring back to the bijection from $J(T_n)$ to $Z^{6V}(n)$ from [22]. Recall from the covering relations of the 20V model that we can think of S_n as replacing each point in T_n with two points a, a' where $a \leq a'$. With the provided Hasse diagram for S_n, we can state this more precisely. Let us contract S_n along the vectors $\vec{w}$ and $\vec{l}$ as follows:

1. Consider all the points that have minimum value in their x-coordinate, and contract the Hasse diagram on these points along all vectors $\vec{w}$.
2. Of the remaining uncontracted points, take those that have minimum value in their z-coordinate, and contract the Hasse diagram on these points along all vectors $\vec{l}$.
3. Of the remaining points, repeats steps 1 and 2 until all points in T_n have been contracted.

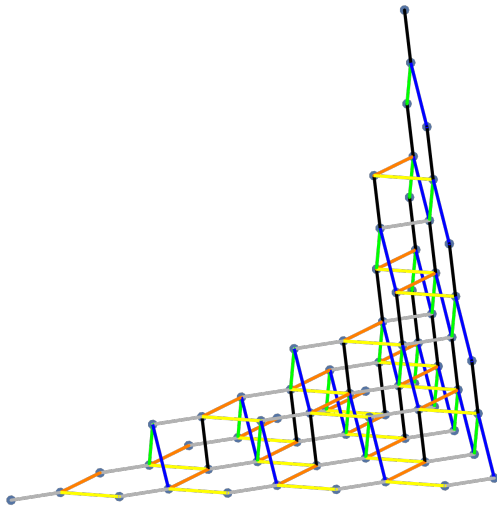

Figure 2.8: The Hasse diagram for the poset S_6. In addition to the colors in Figure 2.2, $\vec{w}$ corresponds to the grey edges and $\vec{l}$ corresponds to the black edges.

Then the resulting Hasse diagram is exactly that of T_n. In this way for every vertex $a \in T_n$, we can label corresponding vertices $a \leq a'$ in S_n. Then $a \in S_n$ corresponds to the raising a path from a corner to diagonal on the four vertices associated with $a \in T_n$, and $a' \in S_n$ corresponds to the raising a path from the diagonal to the corner on those same four vertices. As a result, the points in any plane $z = k$ for $k \in \mathbb{Z}$ correspond to raising operations of the same path.

From here onward, for any $a \in T_n$, we will use a and a' to refer to those corresponding points in S_n (so that as sets $T_n \subseteq S_n$ and $S_n = T_n \bigcup T'_n$ – see Definition 2.1.7 later). See Figure 2.9. We will restate this in Remark 2.1.6, and refer to this labeling of points in S_n by this remark.

For the 6V model, any point $a \in T_n$ covers up to four other points in T_n by (some subset of) the edges $\{\vec{b}, \vec{g}, \vec{y}, \vec{o}\}$, since the covering relation (Figure 2.4) depends on there being edges to raise (represented by $\vec{b}$ and $\vec{g}$) as well as the edges in the path above having already been raised (represented by $\vec{y}$ and $\vec{o}$). However for the 20V model any point $a \in S_n$ covers up to three other points in S_n either by (some subset of) the edges $\{\vec{b}, \vec{g}, \vec{w}\}$ or by (some subset of) the edges $\{\vec{y}, \vec{o}, \vec{l}\}$. We think of the former case as raising a path from a corner to a diagonal: $\vec{b}$ and $\vec{g}$ represent the path having reached the corner and $\vec{w}$ represents the path above having been raised from the diagonal. Similarly we think of the latter case as raising a path from a diagonal to a corner: $\vec{l}$ represents the path having reached the diagonal and $\vec{y}$ and $\vec{o}$ represent the path above having been raised from the corner. With this, we see that

the covering relations provided by S_n are correct.

Finally to see that $J(S_n)$ actually permits a bijection to $Z^{20V}(n)$ let us induct on n. For small values of n we can check directly that the above bijection works, for example see Figure 2.9. Now from the smallest configuration of $Z^{20V}(n)$, let us apply a number of raising operations. First, perform a raising operation on each segment of each path so that a path consisting of all corners now consists of all diagonal edges, and vice versa. Then fully raise the top-left-most path. The resulting configuration is pictured as the right configuration of Figure 2.11. We see that any more raising operations on this configuration must be done on the central $(n-2)\times(n-2)$ vertices, and can be considered as raising operations on $Z^{20V}(n)$. Hence if we remove the points in S_n corresponding to these raising operations, the resulting poset should be that of S_{n-2}.

Again from Remark 2.1.6, the points corresponding to these raising operations are exactly those points satisfying either $z = 0$ (for the first set of raising operations) or $x = 0$ (for the second set of raising operations). Then it remains to be seen that S_n without these points gives us S_{n-2}. Indeed we see that the resulting poset can be defined exactly as in Proposition 2.1.5 except now we start with the points $(1, 2m+2, 1)$ for $m = 0, \ldots, n-3$. Then applying a change of coordinates

$$(x, y, z) \mapsto (x', y', z') = (x - 1, y - 2, z - 1)$$

we see that our remaining points must satisfy $x' \geq 0$, $z' \geq 0$ and either

$$\begin{cases} 3(x'+1) + 2(y'+2) + (z'+1) \leq 4n - 3 \\ 3(x'+1) - 2(y'+2) + (z'+1) \leq 1 \end{cases} \implies \begin{cases} 3x' + 2y' + z' \leq 4(n-2) - 3 \\ 3x' - 2y' + z' \leq 1 \end{cases}$$

or

$$\begin{cases} (x'+1) + 2(y'+2) + 3(z'+1) \leq 4n - 4 \\ (x'+1) - 2(y'+2) + 3(z'+1) \leq 0 \end{cases} \implies \begin{cases} x' + 2y' + 3z' \leq 4(n-2) - 4 \\ x' - 2y' + 3z' \leq 0 \end{cases}$$

Hence we obtain S_{n-2}, proving our result. □

We restate an important idea from our proof as a remark.

Remark 2.1.6. As seen in the proof of Proposition 2.1.5, for every point $a \in T_n$ there exists points $a, a' \in S_n$ such that a' covers a. Moreover if we contract all the edges corresponding to these covering relations in the Hasse diagram of S_n, we obtain exactly the Hasse diagram of T_n. In particular, every point in S_n can be uniquely identified as a or a' for some $a \in T_n$ as seen in Figure 2.9, and for the rest of this section we will refer to points in S_n in this way.

Recall from Theorem 1.1.10 that Di Francesco and Guitter established a way of sending any configuration of the 20V model to a (or several) configuration of the 6V model. We can use this to construct a map sending every configuration of the 6V model to its preimage

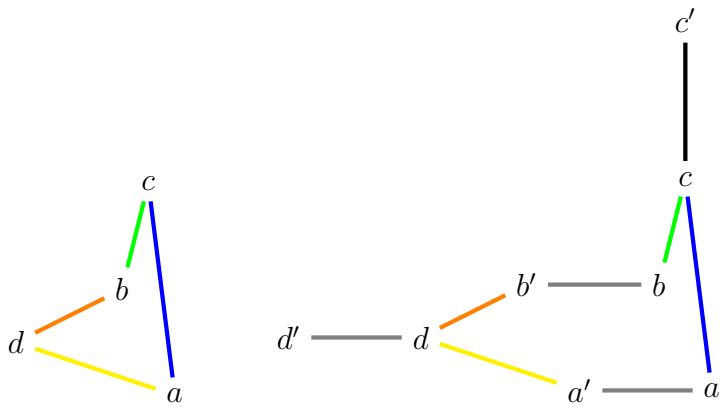

Figure 2.9: Labeling vertices of T_4 and S_4

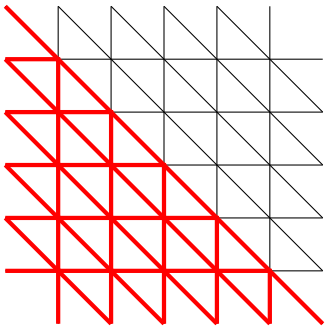

Figure 2.10: The smallest element of $Z^{20V}(5)$.

of 20V model configurations. Moreover since the 6V model and 20 model are in bijection with $J(T_n)$ and $J(S_n)$, respectively, we can define φ to be the map from $J(T_n)$ to subsets of $J(S_n)$.

$$\begin{array}{ccc} Z^{6V}(n) & \longrightarrow & \{\text{subsets of } Z^{20V}(n)\} \\ \updownarrow & & \updownarrow \\ J(T_n) & \xrightarrow{\varphi} & \{\text{subsets of } J(S_n)\} \end{array}$$

We state the map φ in Proposition 2.1.8, but first it will help to make a few definitions.

Definition 2.1.7. For any lower set $I \in J(T_n)$, we will also consider I as a subset of S_n. From Remark 2.1.6, $I \subset S_n$ is exactly those points labeled a for all $a \in I \subseteq T_n$. Note then that I contains no entries labeled a' for any a, and also that $I \subset S_n$ is not necessarily a lower set of S_n.

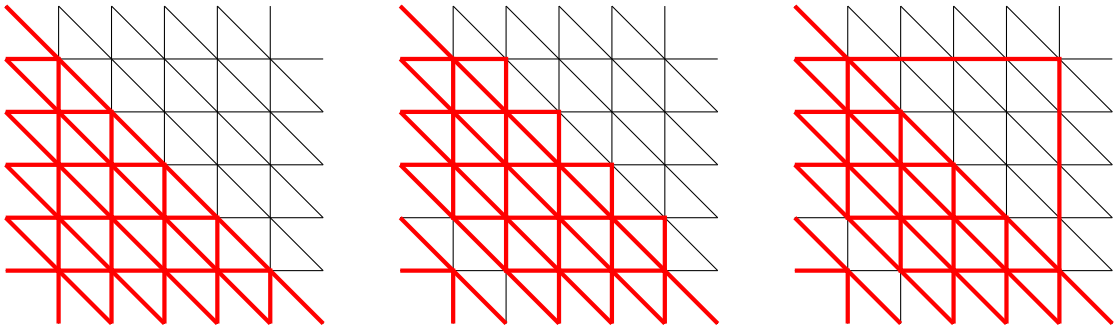

Figure 2.11: The inductive step for Proposition 2.1.5.

For $I \in J(T_n)$ we also define $I' \subset S_n$ defined as $I' = \{a' \in S_n \mid a \in I\}$, so that now I' does not contain any entries labeled a. Again I' is not necessarily or even usually a lower set of S_n.

For any set $U \subseteq S_n$ we define $\overline{U}$ to be the lower set generated by U, that is $\overline{U} = \{x \in S_n \mid$ there exists $y \in U$ such that $x \leq y\}$.

Define T_n^u be the points in T_n that correspond to a raising operation that changes the configuration on at least one edge above the main diagonal $y = n-x$ and below $y = n+1-x$. Then for any $I \in J(T_n)$ we define $I^u = I \bigcap T_n^u$.

Finally define for any $I \in T_n$ the set I^m to be the set of maximal elements of I under the poset structure of T_n.

Proposition 2.1.8. *φ as a map from $J(T_n)$ to intervals of $J(S_n)$ sends for any $I \in J(T_n)$ to the interval of lower sets containing $\overline{I^u}$ and contained in $\overline{I'}$, that is*

$$\varphi : I \mapsto \left\{K \in J(S_n) \mid \overline{I^u} \leq K \leq \overline{I'}\right\}.$$

The intervals in the image of φ are not pairwise disjoint. However if we instead define a map ψ from $J(T_n)$ to intervals of $J(S_n)$ by sending any $I \in J(T_n)$ to the interval of lower sets containing $\overline{I^m}$ and contained in $\overline{I'}$, that is

$$\psi : I \mapsto \left\{K \in J(S_n) \mid \overline{I^m} \leq K \leq \overline{I'}\right\}.$$

Of note we get that the sets in the image of this map are pairwise disjoint. Hence we obtain the following corollary.

Corollary 2.1.9.

$$\sum_{A \in Z^{6V}(n)} |\psi(A)| = |Z^{20V}(n)|$$

for all n.

2.2 Symplectic Tableaux

In this section, we will use the Hasse diagram of S_n to find a bijection from $Z^{20V}(n)$ to pairs of symplectic tableaux subject to some additional constraints. Along the way we will encounter the well known combinatorial object known as Dyck paths:

Definition 2.2.1. A *Dyck path* of order n is a path from $(0,0)$ to (n,n) using north and east steps that does not go below the line $y = x$.

It is well known that Dyck paths are counted by Catalan numbers $C_n = \frac{1}{n+1}\binom{2n}{n}$. Of the many objects also counted by Catalan numbers, let us observe that Dyck paths of order n are in bijection with standard Young tableau of shape (n,n) with entries $\{1,\ldots,2n\}$. The bijection puts places i in the top row of the tableau if the ith step of the Dyck path is north step, and otherwise places i in the bottom row of the tableau if the ith step of the Dyck path is an east step. Figure 2.12 provides a Dyck path of order 5, and its corresponding standard Young tableau under this bijection.

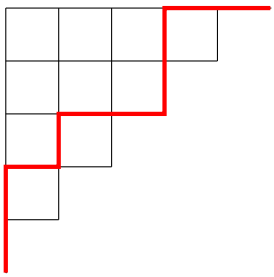

1	2	4	7	8
3	5	6	9	10

Figure 2.12: A Dyck path from $(0,0)$ to $(5,5)$, and the corresponding standard Young tableau of shape $(5,5)$.

Now let us now consider Hasse diagram of S_n with the edges $\vec{w}$ and $\vec{l}$ removed. As pictured in Figure 2.13 the resulting Hasse diagram consists of $2(n-2)$ components that are mutually disconnected – that is elements in different components have no relation under our poset.

Indeed, if we consider the definition of S_n from Proposition 2.1.5 we see that each component of the resulting Hasse diagram necessarily consists of alternating layers of edges in $\{\vec{b},\vec{g}\}$ and $\{\vec{y},\vec{o}\}$. Furthermore if two points in $a_1, a_2 \in S_n$ differ by either $\vec{w}$ or $\vec{l}$ then there does not exist $c_{i,j} \in \mathbb{Z}_{\geq 0}$ for $i = 1,2$ and $j = 1,2,3,4$ such that

$$a_1 + c_{1,1}\vec{b} + c_{1,2}\vec{g} + c_{1,3}\vec{y} + c_{1,4}\vec{o} = a_2 + c_{2,1}\vec{b} + c_{2,2}\vec{g} + c_{2,3}\vec{y} + c_{2,4}\vec{o}$$

and $|(c_{i,1} + c_{i,2}) - (c_{i,3} + c_{i,4})| \leq 1$ for both $i = 1,2$.

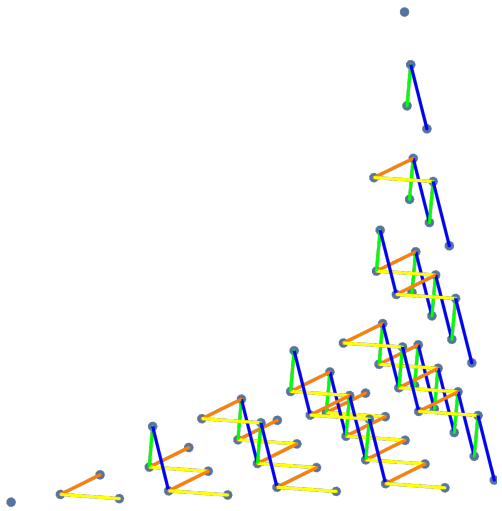

Figure 2.13: Only the relations corresponding to $\vec{b}, \vec{g}, \vec{y}, \vec{o}$ for the Hasse diagram for the poset S_6.

From Remark 2.1.6, each component corresponds to raising operations that change the vertical or horizontal edges between the lines $y = k - x$ and $y = k + 1 - x$ for some k.

Now each of these components contains a maximal element a, and the entire component consists of points

$$a - c_1\vec{b} - c_2\vec{g} - c_3\vec{y} - c_4\vec{o}$$

where $c_1, c_2, c_3, c_4 \in \mathbb{Z}_{\geq 0}$, $c_1 + c_2 + c_3 + c_4 \leq m$ for some m, and $(c_1 + c_2) - (c_3 + c_4) \in \{0, 1\}$ or $(c_1 + c_2) - (c_3 + c_4) \in \{-1, 0\}$ depending on the component. In particular, as pictured in Figure 2.13, each component is a "triangular" Hasse diagram. Then with the observation that lower sets of each of these components are in bijection with Dyck paths (in particular, with a Dyck path that begins two rows below the Hasse diagram and exactly has those points of the lower set below it), we have the following proposition.

Proposition 2.2.2. *Lower sets of the Hasse diagram of S_n with only the relations given by $\vec{b}, \vec{g}, \vec{y}, \vec{o}$ are in bijection with*

$$P_1^2 \times P_2^2 \times \cdots \times P_n^2$$

where P_k is the set of subsets of $\{1, \ldots, 2k-1\}$ of size k containing 1.

Proof. The proof is mostly stated above, but also recall that Dyck paths of order n are in bijection with standard Young tableau of shape (n, n), which are completely determined by their top row. Then since lower sets of each component of the Hasse diagram are in bijection

with Dyck paths, specifically for each $k = 1, \ldots, n$ there are two components whose lower sets are in bijection with Dyck paths of order k, we have our result. □

Furthermore in the Hasse diagram of S_n with only the relations given by $\vec{b}, \vec{g}, \vec{y}, \vec{o}$, we see that there are two types of connected components: those starting with one of $\vec{b}, \vec{g}$ or those starting with one of $\vec{y}, \vec{o}$. Indeed, those with of the former type lie in the closed half-space $x \geq z$, and those of the latter type lie in its complement $x < z$. With this distinction, we see that the bijection in Proposition 2.2.2 may be made with

$$(P_1 \times P_2 \times \cdots \times P_n)^2$$

with one copy of $\mathcal{P}_n^1 := P_1 \times \cdots \times P_n$ corresponding to the part of S_n satisfying $x \geq z$, and one copy of $\mathcal{P}_n^2 := P_1 \times \cdots \times P_n$ corresponding to $x < z$.

First let us consider $\mathcal{P}_n^1$ and the skew shape $(n, \ldots, n)/(n-1, n-2, \ldots, 1, 0)$. For each column of length k in the skew shape, we fill it with a subset of $\{1, \ldots, 2k-1\}$ of size k containing 1, so that the column is strictly decreasing. In this way, fillings of our skew shape are in bijection with $\mathcal{P}_n^1$.

Now we wish to restrict $\mathcal{P}_n^1$ so that our bijection can be made with all the lower sets of the half of S_n satisfying $x \geq z$, including the relations given by $\vec{w}$ and $\vec{l}$. Of course, we do this by introducing the relations imposed by $\vec{w}$ and $\vec{l}$ into what we already have. It will help to define a number of somewhat unusual operations.

Definition 2.2.3. For any integer x, we define

- $\lfloor x \rfloor_{\text{even}}$ to be the greatest even integer less than or equal to x
- $\lceil x \rceil_{\text{even}}$ to be the least even integer greater than or equal to x
- $\lceil x \rceil_{\text{odd}}$ to be the least odd integer greater than or equal to x

Then introducing the relations given by $\vec{w}$ requires us to impose $z \leq \lfloor y \rfloor_{\text{even}}$, where y, z are any two entries a knight's move away as pictured in Figure 2.14. Next, introducing $\vec{l}$ requires us to impose $x \leq \lceil z+1 \rceil_{\text{odd}}$, where x, z are any two entries diagonally adjacent as pictured in Figure 2.14.

Similarly, $\mathcal{P}_n^2$ is also in bijection with fillings of the skew shape $(n, \ldots, n)/(n-1, n-2, \ldots, 1, 0)$ with the same restrictions on the entries in columns as above. Moreover the relations given by $\vec{w}$ and $\vec{l}$ are exactly those of $\vec{l}$ and $\vec{w}$ in $\mathcal{P}_n^1$, respectively. Hence lower sets of the half of S_n satisfying $x < z$ are also in bijection with fillings of the skew shapes with the conditions $z \leq \lfloor y \rfloor_{\text{even}}$ and $x \leq \lceil z+1 \rceil_{\text{odd}}$ as before.

Finally we can obtain a bijection to all lower sets of S_n from pairs of fillings of skew shapes. Each filling is subject to all the conditions above, with additional constraints given by the relations imposed by those $\vec{w}$ and $\vec{l}$ which involve points on the plane $x = z$. We observe that these relations are only between the largest connected component in each of $x \geq z$ and $x < z$, which corresponds to P_n in each of $\mathcal{P}_n^1$ and $\mathcal{P}_n^2$. Then in terms of the

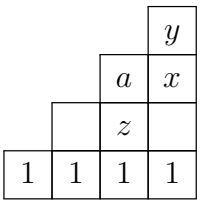

Figure 2.14: The skew shape corresponding to $\mathcal{P}_4^1$ and $\mathcal{P}_4^2$.

our pair of skew shapes, the only conditions we have are on the rightmost columns of each shape. Specifically we have from the relations $\vec{l}$ the condition $x \leq \lceil y \rceil_{\text{even}}$ for any x, y from the same row with x coming from the skew shape corresponding to $\mathcal{P}_n^1$ and y coming from the skew shape corresponding to $\mathcal{P}_n^2$. Similar to before we use $\lceil y \rceil_{\text{even}}$ to denote the smallest even integer greater than or equal to y. We also have from the relations $\vec{w}$ the condition $y \leq \lceil z \rceil_{\text{even}}$ where z is from the skew shape corresponding to $\mathcal{P}_n^1$, y is from the skew shape corresponding to $\mathcal{P}_n^2$, and z is in the row above y. Both of these conditions are pictured in Figure 2.15.

This gives us the proposition below. Going forward, we will use this bijection with pairs of skew shapes without identifying one skew shape as corresponding to $\mathcal{P}_n^1$ and the other as corresponding to $\mathcal{P}_n^2$.

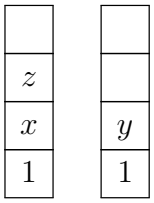

Figure 2.15: For our bijection to all lower sets of S_n, the rightmost column in each skew shape must satisfy $x \leq \lceil y \rceil_{\text{even}}$ and $y \leq \lceil z \rceil_{\text{even}}$ for any x, y, z as pictured above with the column from $\mathcal{P}_4^1$ on the left.

Proposition 2.2.4. *Lower sets of S_n are in bijection with fillings of a pair of skew shapes $(n, \ldots, n)/(n-1, \ldots, 0)$ such that in each of the skew shapes we have the relations*

$$x < y, \quad x \leq \lceil z + 1 \rceil_{odd}, \quad z \leq \lfloor y \rfloor_{even}$$

for any x, y, z as pictured in Figure 2.14, and for the two rightmost columns we have

$$x \leq \lceil y \rceil_{even}, \quad y \leq \lceil z \rceil_{even}$$

for any x, y, z as pictured in Figure 2.15.

Let us also observe that the rows in both skew shapes are weakly decreasing. Consider any a, x, y, z as pictured in Figure 2.14. We will show that $a \geq x$. If a is even, then the conditions in Proposition 2.2.4 give us that $y \leq \lceil a+1 \rceil_{\text{odd}} = a+1$. Then $x < y \leq a+1 \implies x \leq a$ as desired. On the other hand if a is odd then $z < a$ and $x \leq \lceil z+1 \rceil_{\text{odd}} \leq z+1 \leq a$, again as desired.

Now if we substitute the integers in our filling of our skew shapes with entries $1 < \overline{1} < 2 < \cdots < \overline{n-1} < n$ via

$$i \mapsto \begin{cases} \overline{n - \frac{i}{2}} & i \text{ even} \\ n - \frac{i-1}{2} & i \text{ odd} \end{cases}$$

then we see that each of the fillings of our skew shapes are now weakly increasing in rows, strictly increasing in columns, and i and $\bar{\imath}$ do not appear past the ith row. Note that this third property comes from the fact that the kth column contains only integers in $\{1, \ldots 2k-1\}$ and hence only entries in $\{n+1-k, \overline{n+1-k}, \ldots, n\}$. With these three conditions, we see that these are pairs of symplectic skew tableaux, with some extra conditions, as outlined in below.

Theorem 2.2.5. *Lower sets of S_n are in bijection with pairs of symplectic skew tableaux of shape $(n, \ldots, n)/(n-1, n-2, \ldots, 1, 0)$ such that in each skew tableaux for any x, y, z as pictured in Figure 2.16 we have*

$$x \geq \lfloor z-1 \rfloor, \quad z \geq \lceil y \rceil$$

and also for the rightmost columns of the two skew tableaux for any x, y, z as pictured in Figure 2.17 we have

$$x \geq \lceil y-1 \rceil, \quad y \geq \lceil z-1 \rceil$$

Here we use $z-1$ to denote the value preceding z, so that $3-1 = \overline{2}$ and $\overline{3}-1 = 3$. Also, we use $\lfloor x \rfloor$ to denote the unbarred value corresponding to x. Similarly we use $\lceil x \rceil$ to denote the barred value corresponding to x. In this way, for both $x = i$ or $x = \bar{\imath}$ we would have

$$\lfloor x \rfloor = i \text{ and } \lceil x \rceil = \bar{\imath}.$$

We give an example of the bijections in Proposition 2.2.4 and Theorem 2.2.5 from a lower set of S_4 in Figure 2.18.

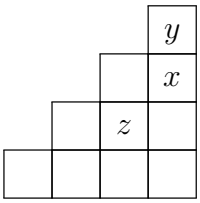

Figure 2.16: For the symplectic skew tableux in Theorem 2.2.5, we also require that any x, y, z as pictured satisfy $x \geq \lfloor z - 1 \rfloor$ and $z \geq \lceil y \rceil$.

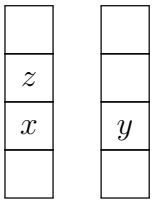

Figure 2.17: For any pair of symplectic skew tableaux in Theorem 2.2.5, we also require that in their rightmost columns any x, y, z as pictured satisfy $x \geq \lceil y - 1 \rceil$ and $y \geq \lceil z - 1 \rceil$.

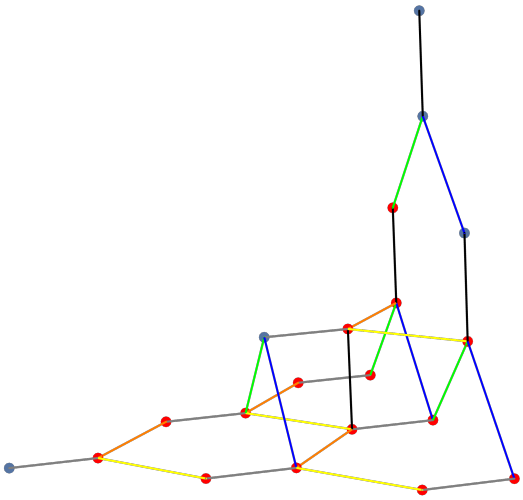

			5
		3	3
	3	2	2
1	1	1	1

			4
		4	3
	3	3	2
1	1	1	1

			2
		3	3
	3	$\overline{3}$	$\overline{3}$
4	4	4	4

			$\overline{2}$
		$\overline{2}$	3
	3	3	$\overline{3}$
4	4	4	4

Figure 2.18: The lower set denoted by the red points in the pictured S_4 and its pairs of skew tableaux and symplectic skew tableaux, according to the bijections in Proposition 2.2.4 and Theorem 2.2.5, respectively.

2.3 Alternating Phase Matrices

Just as the 6V model is in bijection with alternating sign matrices (ASMs) [17] [23], we can create an analogous bijection for the 20V model. Di Francesco and Guitter construct such an object in [9]: alternating phase matrices (APMs).

Definition 2.3.1. An *alternating phase matrix* of size n is an $n \times n$ matrix of entries $(h, v, d) \in \{-1, 0, 1\}^3$ such that

(i) $h_{i,j} + v_{i,j} + d_{i,j} = 0$ for all $i, j \in \{1, \ldots, n\}$

(ii) Each row has a nonzero h and each column has a nonzero v

(iii) Along rows, the nonzero h alternate in sign, beginning with 1 and ending with 1.

(iv) Along columns the nonzero v alternate in sign, beginning with -1 and ending with -1.

(v) Along lower diagonals, including the main diagonal, the nonzero d alternate in sign, beginning with 1 and ending with -1. Along upper diagonals, the nonzero d alternate in sign, beginning with -1 and ending with 1.

We can think of an alternating phase matrix as describing at each vertex of the 20V model whether there is a net incoming (-1), net outgoing (1), or no net (0) horizontal, vertical, and diagonal edge. Of note, the aforementioned and widely known ASMs are realized as APMs where $d_{i,j} = 0$ for all i, j.

Proposition 2.3.2. *Alternating phase matrices are in bijection with pairs of symplectic tableaux from Theorem 2.2.5.*

Proof. In [9] Di Francesco and Guitter actually show that these APMs are in bijection with configurations of the 20V model. By Theorem 2.2.5 and Proposition 2.1.5, it follows that our pairs of symplectic tableaux are also in bijection with APMs. □

Below we will provide one way of explicitly constructing a pair of symplectic tableaux from any APM. Theorem 2.2.5 and Proposition 2.1.5 together give us an explicit bijection from the 20V model to pairs of symplectic tableaux (subject to our extra conditions), so if we can reconstruct the configuration of the 20V model from our APM, we can write this bijection.

Given an APM $((h_{i,j}, v_{i,j}, d_{i,j}))_{1 \le i,j \le n}$ we construct two matrices $V \in \{0,1\}^{(n+1)\times n}$ and $H \in \{0,1\}^{n\times(n+1)}$ as follows:

$$V_{i,j} = \begin{cases} \sum_{k=1}^{i} h_{k,j} + d_{k,j} & i = 1, \ldots, n \\ 0 & i = 0 \end{cases}$$

$$H_{i,j} = \begin{cases} \sum_{k=1}^{j} v_{i,k} + d_{i,k} & j = 1, \ldots, n \\ 1 & j = 0 \end{cases}$$

Our matrices V and H encode exactly where the vertical and edges of a configuration of the 20V model occur. In this way, our matrix V ends in a row of 1 and our matrix H ends in a column of 0. These properties can be checked from the definition of APMs.

The matrices V and H completely determine our configuration of the 20V model, but we can also encode the diagonal edges simiarly in a matrix D. Let D be an $n \times n$ matrix in $\{0, 1\}$ defined recursively by

$$D_{i,j} = V_{i-1,j} + H_{i,j-1} + D_{i-1,j-1} - V_{i,j} - H_{i,j}$$

for all $1 \leq i, j \leq n$. Then $D_{i,j}$ records whether or not the vertex (i, j) in a configuration of the 20V model has an outgoing diagonal edge. This allows us to characterize exactly which $(V, H) \in \{0, 1\}^{(n+1)\times n} \times \{0, 1\}^{n\times(n+1)}$ arise from a valid APM. These are exactly when $D_{i,j}$ as defined above satisfy

- $D_{i,j} \in \{0, 1\}$ for all $1 \leq i, j \leq n$
- $D_{n,j} = 1$ for all $1 \leq j \leq n$
- $D_{i,n} = 0$ for all $1 \leq i \leq n - 1$

In any case, with the configuration of the 20V model recovered from an APM, we return now to our explicit bijection. For $i \geq j$:

- If $V_{i-1,j} = 0$ then column $n - i + j$ of the right tableau has an entry $\overline{n - j}$.
- If $H_{i,j} = 1$ then column $n - i + j$ of the right tableau has an entry $n - j$.

Otherwise for $i < j$:

- If $H_{i,j-1} = 1$ then column $n - j + i$ of the left tableau has an entry $\overline{n - i}$.
- If $V_{i,j} = 0$ then column $n - j + 1$ of the left tableau has an entry $n - i$.

Sorting entries in each column in ascending order gives us the pair of symplectic tableaux.

Figure 2.19 gives an example of the bijection from APM to $Z^{20V}(n)$ to pairs of symplectic tableaux, as well as the corresponding matrices V, H, and D.

2.4 Conclusion

We have now identified several bijections for the 20V model with the boundary condition DWBC1, as defined in Definition 1.1.9. Each of these bijections has an analogous bijection with the 6V model, and as such these served as an initial attempt to find a nice product formula for the 20V model akin to the well known formula for enumerating 6V model configurations

$$\prod_{i=0}^{n-1} \frac{(3i+1)!}{(n+i)!}$$

$$\begin{pmatrix} (0,-1,1) & (0,0,0) & (1,-1,0) \\ (0,0,0) & (1,0,-1) & (0,0,0) \\ (0,0,0) & (1,-1,0) & (0,0,0) \end{pmatrix}$$

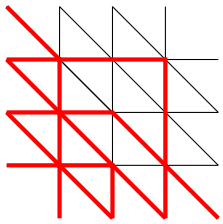

$$V = \begin{pmatrix} 0 & 0 & 0 \\ 1 & 0 & 1 \\ 1 & 0 & 1 \\ 1 & 1 & 1 \end{pmatrix} \quad H = \begin{pmatrix} 1 & 1 & 1 & 0 \\ 1 & 1 & 0 & 0 \\ 1 & 1 & 0 & 0 \end{pmatrix} \quad D = \begin{pmatrix} 0 & 0 & 0 \\ 1 & 1 & 0 \\ 1 & 1 & 1 \end{pmatrix}$$

		$\overline{2}$
	$\overline{2}$	$\overline{2}$
3	3	3

		$\overline{1}$
	2	2
3	3	3

Figure 2.19: An APM, its corresponding configuration of the 20V model, the matrices V, H, D, as well as the corresponding pair of symplectic tableaux.

Alas in the following Section 3, we see that a multiplicative formula for the 20V model can be obtained by expanding to a larger non-square domain. Still, the question of enumerating 20V model configurations on this square domain remains, and a formula can still possibly be found through one of these combinatorial objects.

Of note, tableaux with a symplectic condition seems to be a key property for the 20V model on any domain and boundary condition. Indeed in Chapter 3 when we examine the 20V model on a different domain, as defined in Definition 1.1.11, we again can establish a bijection to fillings of Young diagrams with a symplectic condition. Admittedly the presence of the somewhat unusual condition on our symplectic skew tableaux in Theorem 2.2.5 makes this enumeration difficult. However the symplectic condition seems to capture something fundamental about the 20V model.

Chapter 3

Domino Tilings

This section is largely based off of [6], which examines the 20V model on trapezoidal domains $\mathcal{T}_n$ from Definition 1.1.11. In particular, in [8] Di Francesco shows that the number of configurations of the 20V model on $\mathcal{T}_n$ is equal to the number of domino tilings on some Aztec triangle, an example of which is pictured in Figure 3.1. He also conjectures that the number of 20V model configurations on $\mathcal{T}_n$ is given by the product formula

$$2^{n(n-1)/2} \prod_{i=0}^{n-1} \frac{(4i+2)!}{(n+2i+1)!}$$

In this section we will construct a domain that generalizes the aforementioned Aztec triangle, and present a generalized product formula in Theorem 3.4.3 to the one conjectured by Di Francesco.

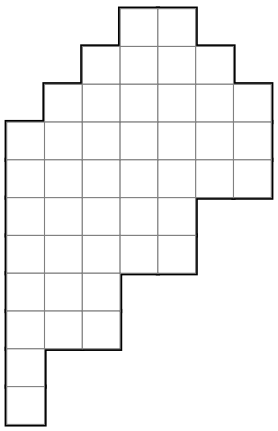

Figure 3.1: An example of an Aztec Triangle considered by Di Francesco in [8] whose domino tilings are equal in number to 20V configurations on $\mathcal{T}_4$.

3.1 Sequences of partitions

First we define certain sequences of partitions, with conditions similar to those found in [2] and [3].

Definition 3.1.1. Given a partition $\mu = (\mu_1, \ldots, \mu_n)$, an integer $m \geq \mu_1$, and a word $w = (w_1, \ldots, w_{2n-1}) \in \{+, -\}^{2n-1}$ or $w = (w_1, \ldots, w_{2n}) \in \{+, -\}^{2n}$, consider sequences of partitions $\lambda^{(0)}, \ldots, \lambda^{(2n-1)}$ or $\lambda^{(0)}, \ldots, \lambda^{(2n)}$, respectively, such that

(1) $\lambda^{(0)}$ is empty

(2) $\lambda^{(2n-1)} = \mu$ or $\lambda^{(2n)} = \mu$, respectively

(3) $\lambda^{(2i+1)}/\lambda^{(2i)}$ is a horizontal strip if $w_{2i+1} = +$ and $\lambda^{(2i)}/\lambda^{(2i+1)}$ is a horizontal strip if $w_{2i+1} = -$

(4) $\lambda^{(2i)}/\lambda^{(2i-1)}$ is a vertical strip if $w_{2i} = +$ and $\lambda^{(2i-1)}/\lambda^{(2i)}$ is a vertical strip if $w_{2i} = -$

(5) $\lambda^{(i)}$ has at most $\lceil \frac{i}{2} \rceil$ nonzero parts

(6) $\lambda^{(i)}_j \leq m$ for all i, j

We will refer to sequences $\lambda^{(0)}, \ldots, \lambda^{(2n-1)}$ as *Case 1*, and sequences $\lambda^{(0)}, \ldots, \lambda^{(2n)}$ as *Case 2*.

Remark 3.1.2. When $w_{2j+1} = +$ for all j, then condition (6) imposes no restriction for m sufficiently large. Specifically, this happens when $m \geq \mu_1 + \#\{j \mid w_{2j} = -\}$. This is because for all i, j we have $\lambda_i^{(2j+1)} - \lambda_i^{(2j)} \geq 0$ and $\lambda_i^{(2j)} - \lambda_i^{(2j-1)} \in \{0, 1\}$ if $w_{2j} = +$ otherwise $\lambda_i^{(2j)} - \lambda_i^{(2j-1)} \in \{-1, 0\}$ if $w_{2j} = -$. Then since $\mu_i \leq \mu_1$ for all i, we see that $\mu_i \leq \mu_1 + \#\{j \mid w_{2j} = -\}$ for all i.

Unless stated otherwise, we will assume $m = \mu_n + \#\{w_{2j} = -\}$.

Delannoy paths

Definition 3.1.3. For any $i, j \in \mathbb{Z}$ the *Delannoy number* $D(i, j)$ is the number of paths from $(0, 0)$ to (i, j) using only north, northeast, or east steps.

Remark 3.1.4. The Delannoy numbers $D(i, j)$ [5] can also be defined recursively by

1. $D(i, j) = 0$ if $i < 0$ or $j < 0$
2. $D(0, 0) = 1$
3. $D(i, j) = D(i - 1, j) + D(i, j - 1) + D(i - 1, j - 1)$

Definition 3.1.5. For $i, j \in \mathbb{Z}$ we also define *H-Delannoy* $H(i, j)$ given by

1. $H(i,j) = 0$ if $i < 0$ or $j < 0$
2. $H(0,-1) = 1$
3. $H(i,j) = 2D(i-1,j) + H(i,j-1)$

We can also interpret $H(i,j)$ as paths – $H(i,j)$ is the number of paths from $(0,0)$ to $(i,j+1)$ using north, northeast, or east steps that do not pass through $(i-1,j+1)$ as shown in Figure 3.2. A number of identities exist for D and H.

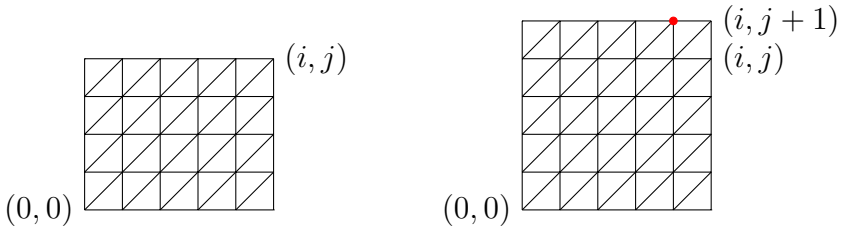

Figure 3.2: On the left, the paths counted by $D(i,j)$ are those from $(0,0)$ to (i,j) taking only north, northeast, and east steps. On the right, the paths counted by $H(i,j)$ are those from $(0,0)$ to $(i,j+1)$ using north, northeast, and east steps that do not pass through the point $(i-1,j+1)$ in red.

Proposition 3.1.6.

$$D(i,j) = D(i-1,j) + H(i,j-1) \tag{3.1}$$
$$= \sum_{m=0}^{i} H(m,j-1) \tag{3.2}$$
$$= \sum_{m} \binom{i}{m}\binom{j}{m} 2^m \tag{3.3}$$
$$H(i,j) = H(i-1,j) + H(i,j-1) + H(i-1,j-1) \tag{3.4}$$
$$= 2\sum_{m=0}^{j-1} D(m,i) \tag{3.5}$$
$$= \sum_{m} \binom{i-1}{m-1}\binom{j+1}{m} 2^m \text{ for } i \geq 1 \tag{3.6}$$

Proof. If we consider the geometry of Definition 3.1.3 and the observation above, equation (1) is clear. Equation (2) then follows by induction on i. To see equation (3), we first observe that $\binom{i}{m}\binom{j}{m}$ is the number of paths from $(0,0)$ to (i,j) using only east and north steps that

have exactly m turns consisting of an east step followed by a north step. Then to count Delannoy paths, we obtain a factor of 2^m since at each of these turns we can instead take a northeast step.

Now equation (1) gives us $H(i,j) = D(i,j+1) - D(i-1,j+1)$, and combined with 3. in Remark 3.1.4 we obtain equation (4). Equation (5) follows from induction on i using 3. in Definition 3.1.5. Finally the proof for equation (6) follows from the argument for equation (3), noting that we are considering paths from $(0,0)$ to $(i,j+1)$ where the east-most column must contain one of the aforementioned east to north turns. □

3.2 Domino Tilings

Definition 3.2.1. Let D be a region of the Euclidean plane that is the union of unit squares whose vertices lie in the integer lattice $\mathbb{Z}^2$. A *domino* is the union of two such unit squares that share an edge. Then we say a *domino tiling* of D is a set $\mathcal{D}$ of mutually disjoint dominoes such that $\bigcup_{d\in\mathcal{D}} = D$.

The goal of this section is to construct domains D such that domino tilings of D are in bijection with Case 1 and Case 2 sequences defined in Definition 3.1.1. These types bijections have been studied many times before [2] [3], and we will use many of the same ideas. But first, let us provide some language to describe our domains which will aid in describing our particular bijection.

Definition 3.2.2. For a domain of unit squares as described in Definition 3.2.1, we number its southwest to northeast diagonals from northwest to southeast, starting with diagonal 0. We will say that these diagonals begin on their southwestern-most square, so that within each diagonal, a squares has its *next* square to its northeast and its *previous* square to its southwest. We can then color the squares of our domain as a chessboard such that even diagonals always consist of light squares. It follows then that our domain is tiled by four types of dominoes as in Figure 3.3. We will refer to the north or west square of a domino as its *start*. Dominoes that start on an even diagonal will be called *even*, and dominoes that start on an odd diagonal will be called *odd*, as in Figure 3.3.

For a domino tiling of a domain, we obtain a sequence of partitions as follows: Even dominoes are filled with holes and odd dominoes are filled with particles (see Figure 3.3). The last diagonal may contain squares not in our domain, in which case we treat those squares as the start of a domino, for example as in Figure 3.4. Then the ith diagonal determines the ith partition $\lambda^{(i)}$ via the following rule: the jth part $\lambda^{(i)}_j$ of this partition is exactly the number of holes to the southwest of the jth-to-last particle.

Remark 3.2.3. Each partition here is obtained via its Maya diagram. A Young diagram, and hence a partition, is determined by the edges that form its southeast boundary. In particular this will be a series of north and east steps beginning with the southwest point of the bottom row of the Young diagram. In this way, for each diagonal in a domino tiling of

our domain D, we obtain a partition by treating holes as east steps and particles as north steps.

Moreover on each diagonal, we can treat the infinite sequence of squares to the southwest not in our domain as having particles, and the infinite sequence of squares to the northeast not in our domain as having holes. See Figure 3.5.

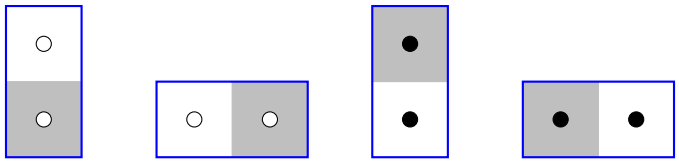

Figure 3.3: Four types of dominoes used to tile our domains, and the resulting holes or particles. The first two types of dominoes are even dominoes, and the last two types of dominoes are odd dominoes. For each domino, its starting square is either its north or west square.

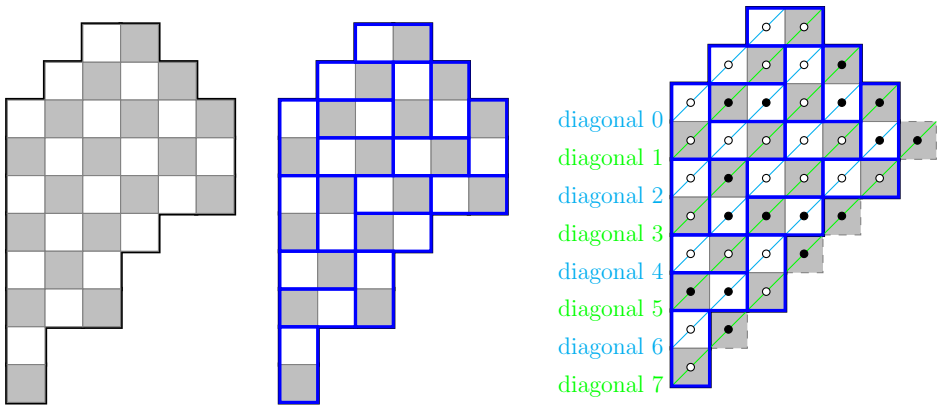

Figure 3.4: A particular domain, a domino tiling on that domain, and a filling of that domino tiling with holes and particles. The corresponding sequence of partitions is $\lambda^{(0)} = (0,0,0,0)$, $\lambda^{(1)} = (1,0,0,0)$, $\lambda^{(2)} = (2,0,0,0)$, $\lambda^{(3)} = \lambda^{(4)} = \lambda^{(5)} = (3,1,0,0)$, $\lambda^{(6)} = (3,2,1,0)$, $\lambda^{(7)} = (3,2,2,1)$.

Case 1 sequences

Recall that for any partition $\mu = (\mu_1, \ldots, \mu_n)$, $m \geq \mu_1$, and $w = (w_1, \ldots, w_{2n-1}) \in \{+,-\}^{2n-1}$, Case 1 sequences are sequences of partitions $\lambda^{(0)}, \ldots, \lambda^{(2n-1)}$ such that

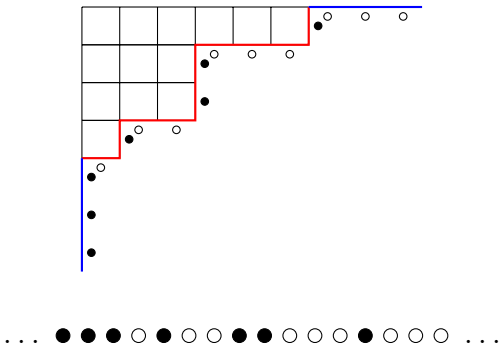

Figure 3.5: The Young diagram for the partition $(6, 3, 3, 1)$ and its Maya diagram. Its shape is completely determined by the north and east steps in red. We can also consider this as an infinite sequence of north and east steps by prepending the blue north steps and appending the blue east steps.

(1) $\lambda^{(0)}$ is empty

(2) $\lambda^{(2n-1)} = \mu$

(3) $\lambda^{(2i+1)}/\lambda^{(2i)}$ is a horizontal strip if $w_{2i+1} = +$ and $\lambda^{(2i)}/\lambda^{(2i+1)}$ is a horizontal strip if $w_{2i+1} = -$

(4) $\lambda^{(2i)}/\lambda^{(2i-1)}$ is a vertical strip if $w_{2i} = +$ and $\lambda^{(2i-1)}/\lambda^{(2i)}$ is a vertical strip if $w_{2i} = -$

(5) $\lambda^{(i)}$ has at most $\lceil \frac{i}{2} \rceil$ nonzero parts

(6) $\lambda^{(i)}_j \leq m$ for all j

Theorem 3.2.4. *The domain D whose domino tilings are in bijection with Case 1 sequences for a given $\mu = (\mu_1, \ldots, \mu_n)$, $m \geq \mu_1$, and $w = (w_1, \ldots, w_{2n-1}) \in \{+, -\}^{2n-1}$ can be constructed by its diagonals as follows:*

(i) Diagonal 0 is of length m.

(ii) The length of each odd diagonal $2i + 1$ is one more than the length of the previous diagonal $2i$. The first (ie. left-most) square of diagonal $2i + 1$ lies

- *Directly below the first square of diagonal $2i$ if $w_{2i+1} = +$*
- *Directly below the first square of diagonal $2i$ if $w_{2i+1} = -$*

(iii) Each even diagonal $2i$ has length equal to the length of the previous diagonal $2i - 1$. The first square of diagonal $2i$ lies

- *Directly below the first square of diagonal* $2i-1$ *if* $w_{2i}=+$
- *Directly to the right of the first square of diagonal* $2i-1$ *if* $w_{2i}=-$

(iv) The last diagonal $2n-1$ *follows (ii) above, but consists of squares in* D *and squares not in* D*: Convert the partition* μ *into its sequence of holes and particles. Then any hole corresponds to a square in* D *and a particle corresponds to a square not in* D*.*

Figure 3.6 shows examples of (iv) in Theorem 3.2.4, and Figure 3.7 illustrates Theorem 3.2.4 for two choices of μ and w (and m taken to be sufficiently large as in Remark 3.1.2).

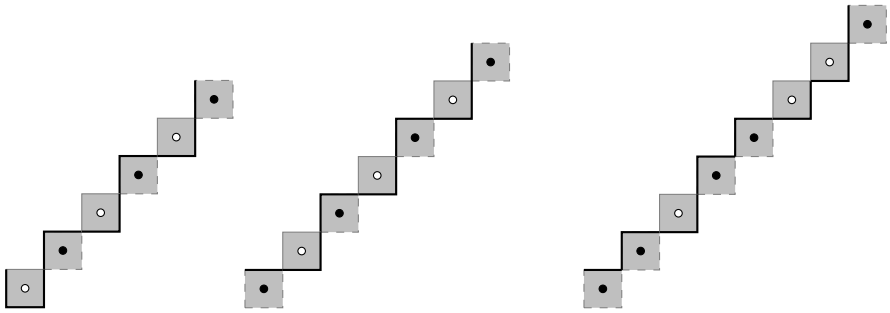

Figure 3.6: On the left, the last diagonal for partition $\mu=(3,2,1)$. In the center $\mu=(3,2,1,0)$, and on the right $\mu=(4,1,1,0,0)$. The resulting southeast boundaries are also drawn.

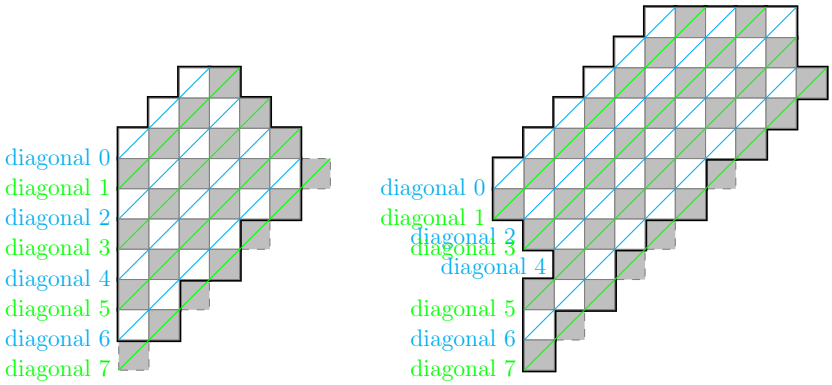

Figure 3.7: On the left, the domain D for the partition $\mu=(3,2,1,0)$ and $w=(+^8)$. On the right, the domain D for the partition $\mu=(3,2,2,1)$ and $w_i=-$ for $i=2,4,5$ and $w_i=+$ otherwise.

Proof. Let us prove first the case where $w = (+^{2n-1})$. We begin by showing that our domain D as defined satisfies our conditions (1)-(6) above. Given that diagonal 0 contains only the start (ie. north or west square) of dominoes, it is clear that (1) must be true. Furthermore due to condition (iv) and since the squares diagonal $2n-1$ that are in D are not starts (ie. only south or east squares) of dominoes, it is clear that (2) must also be true. It can also be seen by induction that each diagonal i has n holes and $\lceil \frac{i}{2} \rceil$ particles, hence we have (5).

Now consider condition (4) when $w_{2i} = +$. Given the configuration of holes and particles on a diagonal $2i-1$, the configuration of holes and particles on diagonal $2i$ is determined by whether the dominoes starting on the previous diagonal are vertical or horizontal. We see that any such vertical domino keeps the particle at the same place from diagonal $2i-1$ to diagonal $2i$, and any horizontal domino moves the particle one square later in the next diagonal. Moreover the restrictions of the domino tiling imply that a horizontal domino requires that any particles immediately following it must also be the start of a horizontal domino. In terms of the corresponding partition this means that going from $\lambda^{(2i-1)}$ to $\lambda^{(2i)}$, each part can increase by at most one with the additional condition that for parts of equal size, if one of these parts increases by one then the earlier parts of equal size must also increase by one. This is exactly the condition that $\lambda^{(2i)}/\lambda^{(2i-1)}$ is a vertical strip.

On the other hand when $w_{2i} = -$, again we consider dominoes that begin on the previous diagonal $2i-1$. The j-to-last domino in diagonal $2i-1$ being horizontal corresponds to $\lambda_j^{(2i)} = \lambda_j^{(2i-1)}$, and the j-to-last domino in the diagonal being vertical corresponds to $\lambda_j^{(2i)} = \lambda_j^{(2i-1)} - 1$. Again a horizontal odd domino forces all subsequent adjacent odd dominoes to be horizontal. Thus $\lambda_j^{(2i-1)}/\lambda_j^{(2i)}$ is a vertical strip. Both cases of w_{2i} are illustrated in Figure 3.8.

For condition (3) we again consider first $w_{2i+1} = +$. In this case, diagonals $2i$ and $2i+1$ begin on the same diagonal just as in our proof for condition (4) when $w_{2i} = +$. Furthermore we see that the configuration of particles on diagonal $2i+1$ is determined by whether the dominoes starting on diagonal $2i$ are vertical or horizontal. However since dominoes starting on diagonal $2i$ contain holes instead of the particles when proving condition (4), we now require

$$\lambda'^{(2i+1)}/\lambda'^{(2i)} \text{ is a vertical strip } \implies \lambda^{(2i+1)}/\lambda^{(2i)} \text{ is a horizontal strip.}$$

Note that since the length of diagonal $2i+1$ is greater than the length of diagonal $2i$, we are permitted to increase the length of $\lambda_n^{(2i)}$.

Now when $w_{2i+1} = -$, the first square of diagonal $2i+1$ is forced to be a particle. We can then obtain a configuration of holes and particles if w_{2i+1} were $+$ by moving this particle to any square of its diagonal strictly to the right of the last particle of diagonal $2i$ as in Figure 3.9. Since removing a horizontal strip is exactly adding a horizontal strip then removing the largest part, we see that $\lambda^{(2i)}/\lambda^{(2i+1)}$ is a horizontal strip as desired. See Figure 3.9.

Hence we have shown that any domino tiling gives us a sequence of partitions as desired. In fact the same argument shows that any sequence of partitions satisfying (1)-(5) must give us a domino tiling of D. In particular conditions (3) and (4) guarantee that we get a domino

tiling of some domain D'. Then condition (5) tells us that the length of each diagonal in this domain D' is the same as in our domain D, and conditions (1) and (2) guarantee that the first and last rows of D' agree with D. This completely determines the shape of D'. $\square$

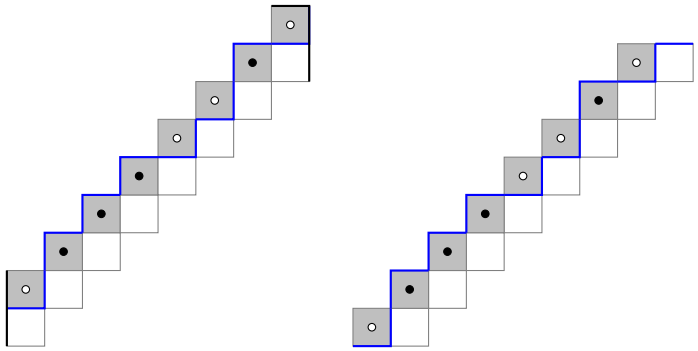

Figure 3.8: Condition (4) for $w_{2i} = +$ on the left and $w_{2i} = -$ on the right, with diagonals $2i-1$ and $2i$. The configuration of holes and particles, hence dominoes, on diagonal $2i$ is completely determined by whether the dominoes beginning on the particles of diagonal $2i-1$ are vertical or horizontal. The blue line denotes how the dominoes must lie based on our configuration of holes and particles.

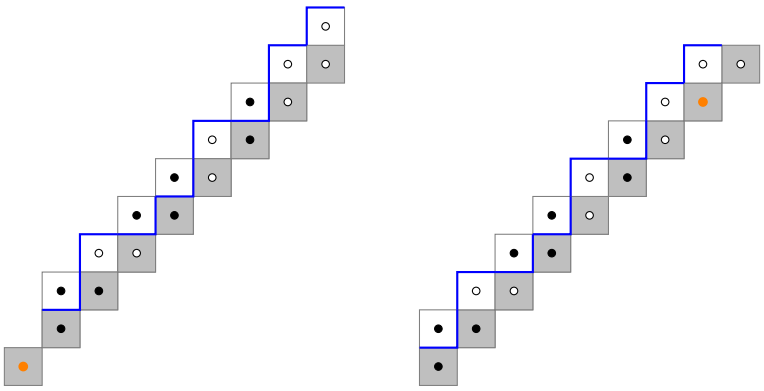

Figure 3.9: Moving the first particle when $w_{2i+1} = -$ to obtain a configuration for $w_{2i+1} = +$. For this particular configuration on diagonal $2i+1$, there are 3 squares to move the orange particle.

Case 2 sequences

The domain on which domino tilings are in bijection with Case 2 sequences can be constructed similarly to that of Case 1 sequences.

Theorem 3.2.5. *The domain D whose domino tilings are in bijection with Case 2 sequences for a given $\mu = (\mu_1, \ldots, \mu_n)$, $m \geq \mu_1$, and $w = (w_1, \ldots, w_{2n}) \in \{+, -\}^{2n}$ can be constructed by its diagonals as follows:*

(i) Diagonal 0 is of length m.

(ii) The length of each odd diagonal $2i+1$ is one more than the length of the previous diagonal $2i$. The diagonal starts so that

- *The first square of diagonal $2i+1$ is directly below the first square of diagonal $2i$ if $w_{2i+1} = +$*
- *The second square of diagonal $2i+1$ is directly below the first square of diagonal $2i$ if $w_{2i+1} = -$*

(iii) Each even diagonal $2i$ has length equal to the length of the previous diagonal $2i-1$. The first square of diagonal $2i$ lies

- *Directly below the first square of diagonal $2i-1$ if $w_{2i} = +$*
- *Directly to the right of the first square of diagonal $2i-1$ if $w_{2i} = -$*

(iv) The last diagonal $2n$ consists of squares in D and squares not in D. Convert the partition μ into its sequence of holes and particles. Then any particles correspond to a square in D and holes correspond to a square not in D.

We illustrate Theorem 3.2.5 with an example in Figure 3.10. Theorem 3.2.5 differs from Theorem 3.2.4 only by (iv), and its proof proceeds similarly.

As mentioned previously, the Aztec triangles in [8] are exactly the Case 1 domains corresponding to the partition $\mu = (n, n-1, \ldots, 1)$ and $w = (+^{2n-1})$. Hence we will refer to these domains, both Cases 1 and 2, as *generalized Aztec triangles*.

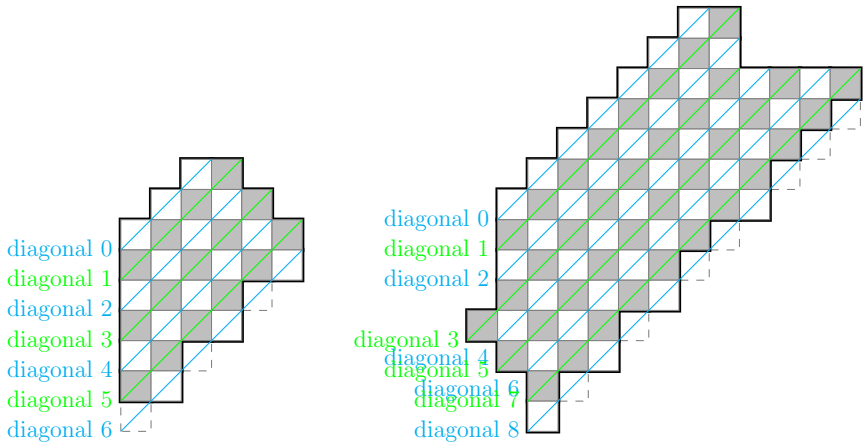

Figure 3.10: On the left, the generalized Aztec triangle D for the partition $\mu = (3, 2, 1)$ and $w = (+^6)$. On the right, the generalized Aztec triangle D for the partition $\mu = (4, 2, 1, 0)$ and $w_t = -$ for $i = 3, 4, 6$ and $w_t = +$ otherwise.

Special cases

Definition 3.2.6. The *Aztec diamond* of order n is the set of unit squares whose vertices lie in the integer lattice $\mathbb{Z}^2$ whose centers (x, y) lie in the region $|x| + |y| \leq n$. See figure 3.11.

It is well known that the number of domino tilings of the Aztec diamond of order n is $2^{n(n+1)/2}$ [10].

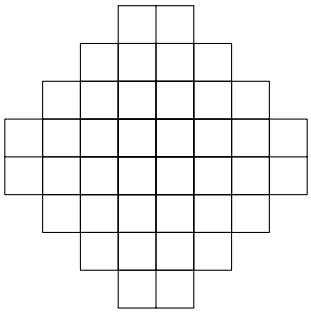

Figure 3.11: The Aztec diamond of order 4.

Corollary 3.2.7. *When $w_{2t} = -$ and $w_{2t+1} = +$ for all t and $\mu = (0^n)$, tilings of the generalized Aztec triangle D are in bijection with tilings of an Aztec diamond. More precisely, tilings of the Case 1 generalized Aztec triangle are in bijection with domino tilings of the Aztec diamond of order $n - 1$, and tilings of the Case 2 generalized Aztec triangle are in bijection*

with domino tilings of the Aztec diamond of order n. It follows then for Case 1 the number of tilings of our domain is $2^{n(n-1)/2}$*, and for Case 2 the number of tilings of our domain is* $2^{n(n+1)/2}$.

Proof. By construction of our generalized Aztec triangle D, when $w_{2t} = -$ and $w_{2t+1} = +$ each diagonal of D ends in the top-most row of D. Moreover since $\mu = (0^n)$, in Case 1 the last diagonal of D contains n squares not in D followed by n squares D. We see then that the i-th row from the top must contain $n + 1 - i$ horizontal (even) dominoes as in Figure 3.12.

On the other hand in Case 2 the last diagonal of D contains n squares in D followed by n squares not in D. Then similarly we see that the i-th row from the top must contain $n - i$ horizontal (even) dominoes, again as in Figure 3.12. In both Cases 1 and 2, if we consider the part of the domain not occupied by these frozen dominoes, we see that what remains is an Aztec diamond. □

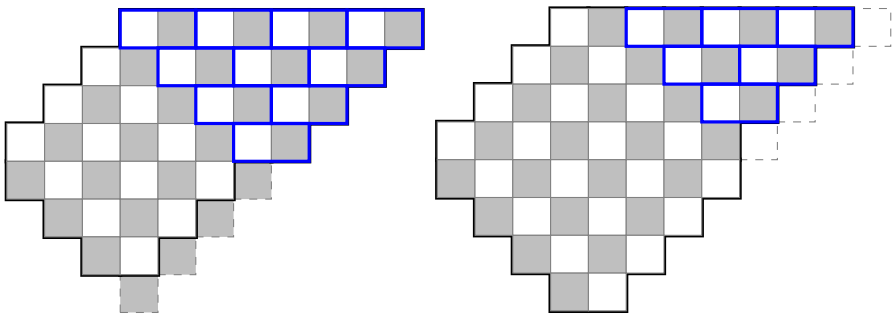

Figure 3.12: The generalized Aztec triangles for Cases 1 and 2, respectively, when $\mu = (0, 0, 0, 0)$, $m = 4$, $w_{2t} = -$ and $w_{2t+1} = +$ for all t. Frozen dominoes are drawn in, and tilings of the domain are exactly tilings of the Aztec diamond.

Corollary 3.2.8. *More generally when* $w_{2i} = -$ *and* $w_{2i+1} = +$ *for all* i *and* μ *is any partition of length* n*, for Case 1 the number of domino tilings is given by* $2^{n(n-1)/2} s_\mu(1^n)$*, and for Case 2 the number of domino tilings is given by* $2^{n(n+1)/2} s_\mu(1^n)$.

Proof. First we consider Case 1. As illustrated in Figure 3.13 the nonfrozen portion of our domain is the northwest part of an Aztec diamond of order $2n-1$ whose southwest boundary is determined by μ. In particular if we consider μ as a series of holes and particles as in Remark 3.2.3 then the southeast-most diagonal includes holes and does not include particles. Since $\mu = (\mu_1, \ldots, \mu_n)$ has particles at $\mu_{n+1-i} + i$, Section 4 in [10] gives us that the number of tilings is

$$2^{n(n-1)/1} \prod_{1 \le i < j \le n} \frac{(\mu_{n+1-j} + j) - (\mu_{n+1-i} + i)}{j - i} = 2^{n(n-1)/2} s_\mu(1, \ldots, 1)$$

Similarly for Case 2, our generalized Aztec triangle is part of an Aztec diamond of order $2n$ where the southeast-most diagonal is determined by μ (again see Figure 3.13). This time it includes particles and does not include holes, but again we can use Section 4 in [10] (also [21] and [3], where these domains are referred to as Aztec rectangles) to see that the number of tilings is

$$2^{n(n+1)/1} \prod_{1 \le i < j \le n} \frac{(\mu_{n+1-j} + j) - (\mu_{n+1-i} + i)}{j - i} = 2^{n(n+1)/2} s_\mu(1, \ldots, 1)$$

□

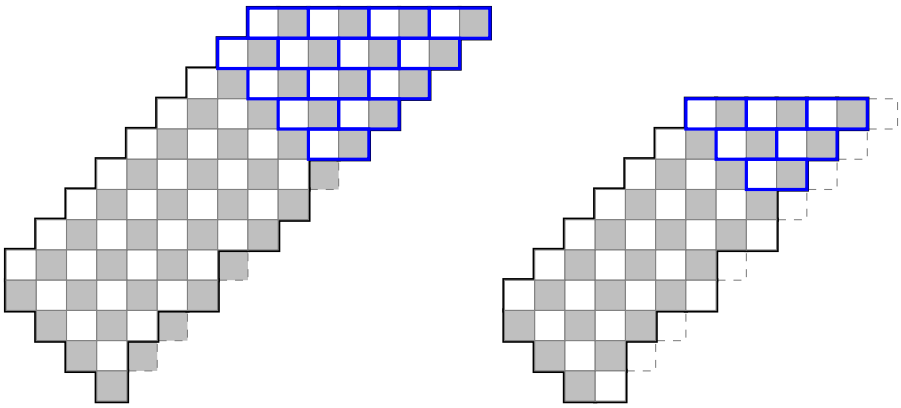

Figure 3.13: Domains when when $w_{2t} = -$ and $w_{2t+1} = +$ for all t with frozen dominoes drawn. Specifically, on the left we have Case 1 for $\mu = (4, 2, 1, 1)$ and on the right Case 2 for $\mu = (3, 2, 0)$.

3.3 Enumeration

Non-intersecting paths

Recall that a Delannoy path is a path from (x_1, y_1) to (x_2, y_2) where $x_1, x_2, y_1, y_2 \in \mathbb{Z}$ using only north, northeast, or east steps. We will say that two Delannoy paths P_1, P_2 are *non-intersecting* if the set of points that P_1 and P_2 pass through are disjoint.

In [8], a bijection between certain non-intersecting Delannoy paths and domino tilings of the Type 1 domains for sequences $\lambda^{(0)} = (0, \ldots, 0), \ldots, \lambda^{(2n-1)} = (n, n-1, \ldots, 1)$ is used to compute the number of domino tilings on these domains. In this section we will prove this bijection, which can be obtained by drawing segments of the paths according to the four types of dominoes, as described in Figure 3.14. These paths end at the penultimate diagonal

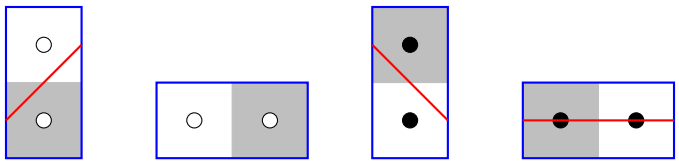

Figure 3.14: For each domino, the path is indicated in red. A parity argument explains why dominoes of the second type do not permit a path.

of our domain, and we consider the paths as being extended southeastward through the last diagonal of our domain, shown in diagonal 7 in Figure 3.15.

For describing our Delannoy paths, it will be helpful to consider a change of coordinates by a rotation of $\frac{\pi}{4}$ and a dilation of $\sqrt{2}$, as well as a translation so that the origin is at the midpoint of the west edge of the first square of diagonal $2n-2$. See Figure 3.15 for this $\mathbb{Z}^2$ lattice after this transformation. For this section we will use east, south, and southeast to describe the direction of steps in these Delannoy paths after this change of coordinates.

Finally, for any word $w \in \{+,-\}^{2n-1}$ or $w \in \{+,-\}^{2n}$, we define $W_i = \#\{w_{2j} = + \mid j > n-i\}$. For example, if $w = (+,+,+,-,+,-,+,+,+)$ so that $w_2, w_8 = +$ and $w_4, w_6 = -$, then $W_1 = 0$, $W_2 = W_3 = W_4 = 1$, and $W_5 = 2$.

Proposition 3.3.1. *Domino tilings on the generalized Aztec triangle corresponding to Case 1 sequences with $w_{2t+1} = +$ for all t are in bijection with non-intersecting n Delannoy paths where the ith path is from $(W_i, i-1)$ to $(\mu_{n-i+1} + i - 1, 0)$*

We present two proofs for this. The first will be a constructive proof allowing us to read the sequence of partitions directly from a set of non-intersecting paths. The second will be a more general proof which we will reference again when we consider other ways of assigning paths to a domino tiling.

Proof of Proposition 3.3.1. The paths permitted by each domino (Figure 3.14) require that the starts of our paths are exactly those dark squares whose left edge lie on the boundary of D. These are exactly the first squares of each odd diagonal. Since these paths always move eastward, they will eventually end on an eastern edge of our domain. Moreover since these paths always leave a domino on a light square, we see that these paths will always exit our domain on the east edge of those squares on the penultimate diagonal whose east edge lies on the boundary of the domain. Equivalently, these are the west edges of the squares on the last diagonal that are not included in our domain. Indeed we observe that for $\mu = (\mu_1, \ldots, \mu_n)$ there are exactly n points where our paths start and n points where our paths end.

By construction via the domino tiling, these n paths will be non-intersecting. Now we claim that this map sending domino tilings to non-intersecting paths is injective. If we label our paths from bottom to top, starting with path 1, we see that the collective number of southeast and east paths in path i must be exactly $i-1$. Hence the location of the odd

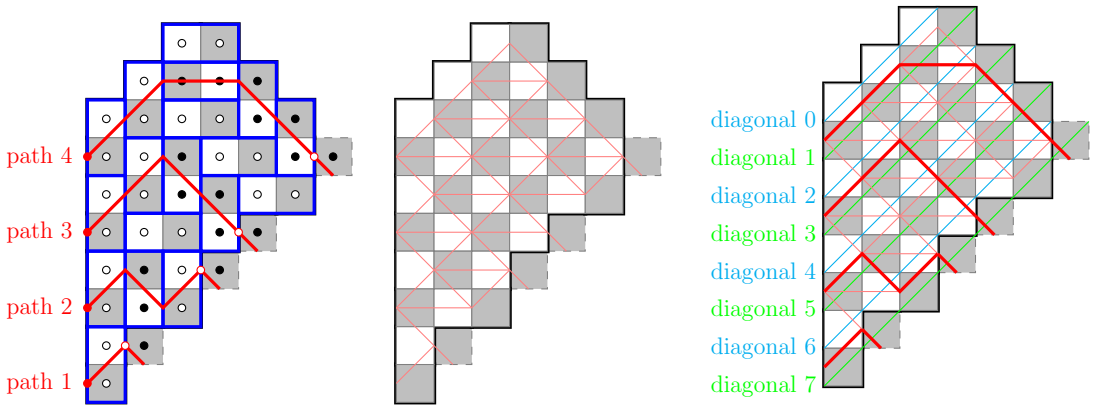

Figure 3.15: A particular domino tiling of the generalized Aztec triangle for Case 1 with $\mu = (3, 2, 2, 1)$ and $w = (+^7)$, and its corresponding Delannoy paths. To the right, the edges on which possible paths can occur for this domain. This vertices of the possible paths lie in the lattice $\mathbb{Z}^2$ after the transformation described above. Corollary 3.3.3 gives the total number of paths, hence tilings, as the determinant

$$\begin{vmatrix} 1 & 1 & 1 & 1 \\ 1 & 5 & 7 & 11 \\ 0 & 5 & 13 & 41 \\ 0 & 1 & 7 & 63 \end{vmatrix} = 704$$

dominoes (that is dominoes with holes) completely determines each path. Then since our previous bijection of domino tilings to sequences of partitions in Section 3.2 gives us that a domino tiling is completely determined by the location of these odd dominoes, our claim is proved.

It remains to be seen that this map from domino tilings to non-intersecting paths is surjective. Since each path i must cross $2(i-1)$ diagonals and each odd domino results in the path crossing 2 diagonals where as each even domino results in the path crossing 0 diagonals, we see that path i contains exactly $i-1$ odd dominoes. As shown above these odd dominoes allow us to recover a sequence of partitions, and we see that $\lambda^{(i)}_{n-j} + \#\{w_t = - \mid t \leq i\}$ is the number of east or northeast steps at least half completed when path j crosses diagonal i.

Then let us check that this sequence of partitions obtained from any set of non-intersecting paths satisfies

(1) $\lambda^{(0)}$ is empty

(2) $\lambda^{(2n-1)} = \mu$

(3) $\lambda^{(2i+1)}/\lambda^{(2i)}$ is a horizontal strip for all i

(4) $\lambda^{(2i)}/\lambda^{(2i-1)}$ is a vertical strip if $w_{2i} = +$ and $\lambda^{(2i-1)}/\lambda^{(2i)}$ is a vertical strip if $w_{2i} = -$ for all i

(5) $\lambda^{(i)}$ has at most $\lceil \frac{i}{2} \rceil$ nonzero parts for all i

(6) $\lambda_j^{(i)} \leq m$ for all i, j

Conditions (1) and (2) are clear, and condition (5) follows from the fact that path i begins between diagonals $2(n-i)$ and $2(n-i)+1$. Condition (6) is follows from the length of each diagonal in our domain.

To observe condition (3), we see that the jth part of $\lambda^{(2i+1)}/\lambda^{(2i)}$ for any j, which we denote as $(\lambda^{(2i+1)}/\lambda^{(2i)})_j$, is determined exactly by the number of east steps taken by path $n-j$ between diagonals $2i+1$ and $2i$. Indeed, $\lambda_j^{(2i+1)}$ and $\lambda_j^{(2i)}$ are determined by the number of east and southeast steps taken by path $n-j$ by diagonal $2i+1$, and any southeast steps cannot have been at least half completed between diagonals $2i$ and $2i+1$. Then noting that at any diagonal, the number of east steps path $n-j-1$ can take is bounded by the total number of east and southeast steps path j has taken, we see that $\lambda^{(2i+1)}/\lambda^{(2i)}$ is a horizontal strip.

A similar argument shows condition (4). Here $\lambda^{(2i)}/\lambda^{(2i-1)}$ is determined by the number of southeast steps taken between diagonals $2i$ and $2i-1$ – either 0 or 1. It is clear that when $w_{2i} = +$, taking a southeast step gives us that $(\lambda^{(2i)}/\lambda^{(2i-1)})_j = 1$ and otherwise $(\lambda^{(2i)}/\lambda^{(2i-1)})_j = 0$. On the other hand, when $w_{2i} = -$, taking a southeast step gives us that $(\lambda^{(2i-1)}/\lambda^{(2i)})_j = 0$ and otherwise $(\lambda^{(2i-1)}/\lambda^{(2i)})_j = 1$. Hence $\lambda^{(2i)}/\lambda^{(2i-1)}$ is a vertical strip if $w_{2i} = +$ and $\lambda^{(2i-1)}/\lambda^{(2i)}$ is a vertical strip. □

And now the second proof of Proposition 3.3.1:

Alternate proof of Proposition 3.3.1. Let us see that any domino tiling of our region must result in a set of n non-intersecting paths as stated. Indeed, each segment of our paths must enter a domino from the west edge of a dark square and exit a domino from the east edge of a light square. It follows that our paths must begin on the dark squares of D whose west edge lies on the boundary of D, and must end on the light squares of D whose east edge lies on the boundary of D.

Conversely, such a set of non-intersecting paths determines the locations of all our dominoes in D except the horizontal even dominoes, that is the domino to which we do not assign any segment of a path. Then it suffices to show that for any two non-intersecting paths, the space in between them can be filled with horizontal even dominoes.

For any two non-intersecting paths, we insert dominoes into our generalized Aztec triangle according to the paths as in Figure 3.16. Then we see that the distance between consecutive paths lines $y = t$ where t is odd (keeping in mind our rotation by $\frac{\pi}{4}$) determines the number of light squares directly above the line $y = t$ that are not filled by dominoes, as well as the number of dark squares directly below the line $y = t$ that are not filled by dominoes. In

particular, each light square of D is not part of a domino must be adjacent to a dark square to its right that is also not part of a domino. Again see Figure 3.16. It follows that the space between any two non-intersecting paths can be filled with horizontal even dominoes.

Note that for dominoes above the north-most path we can consider an additional fixed path as in Figure 3.16. Such a path poses no restrictions on this north-most path, but shows that we can indeed fill the area above this path with horizontal even dominoes. □

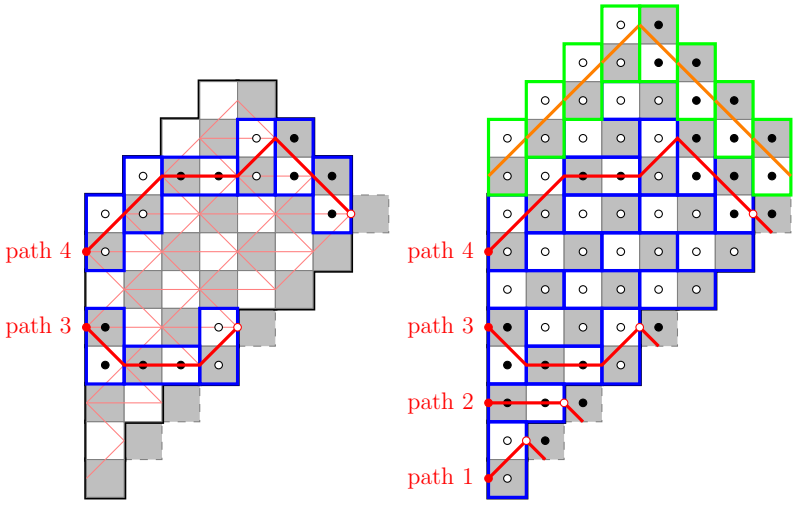

Figure 3.16: On the left, filling the domain with dominoes according to the two paths in red. The green line is a segment of the line $y = 3$ which we use in the second proof of Proposition 3.3.1. Note that between these two paths, there are exactly 3 light squares above the line and 3 dark squares below the line. On the right in green, additional fixed dominoes we add to the domain to show that we can fill the region above the north-most path with vertical dominoes.

Similarly we can identify a bijection from Case 2 sequences when $w_{2i+1} = +$ to sets of non-intersecting Delannoy paths. Again we will use our change of coordinates above to more easily describe where these paths start and end. Of note for Case 2 sequences, the final step in any path cannot an east step, since this would correspond to a change from partition $2n + 1$ to $2n + 2$, but we do not have $\lambda^{(2n+2)}$ for a Case 2 sequence.

Proposition 3.3.2. *Domino tilings on the generalized Aztec triangle corresponding to Case 2 sequences with $w_{2t+1} = +$ for all t are in bijection with non-intersecting n Delannoy paths where the ith path is from $(W_i, i-1)$ to $(\mu_{n-i+1} + i - 1, -1)$ where the last step of each path is not an eastward step.*

Proof. We can use much of our proof for Proposition 3.3.1 to prove this proposition. We need only to justify the different ending points, as well as the additional restriction on the last step of each path.

As with Case 1 sequences, our paths must start at the first square of each odd diagonal and exit at the light squares of D whose right edge lies on the boundary of D. For the generalized Aztec triangles D corresponding to Case 2 sequences, these light squares are exactly the light squares in diagonal $2i$. Hence these paths end at the points $(\mu_{n-i}+i-1,-1)$ for $i=1,\ldots,n$ as desired.

Moreover since these light squares on the final diagonal of D, they cannot be adjacent to a dark square below them. Hence the last step of each path cannot be an eastward step (the first domino in Figure 3.14). □

We note that unlike in the case of Case 2 sequences, there is no restriction on the last step of each path for Case 1 sequences. Indeed, suppose the shape of our generalized Aztec triangle D does not allow some path j to end with an eastward step, that is if some light square in diagonal $2n-2$ which contains the endpoint of some path does not have a dark square below it. Then it must be that the previous path $j-1$ ends at the preceding light square in diagonal $2n-2$ and the non-intersecting nature of our paths will prohibit path j ending with an eastward step. See paths 2 and 3 in Figure 3.15, which illustrate this idea.

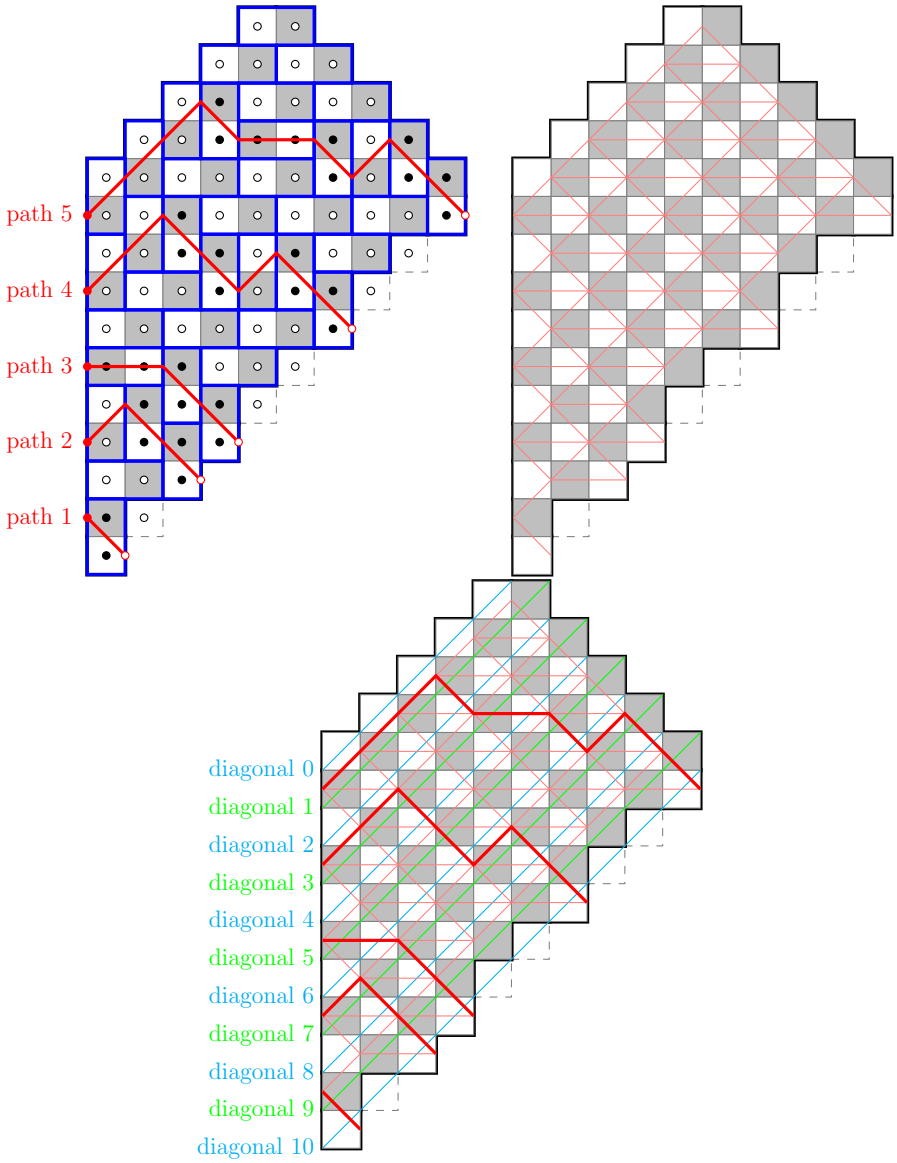

Figure 3.17: A particular domino tiling of the generalized Aztec triangle for Case 2 with $\mu = (5, 3, 1, 1, 0)$ and $w = (+^{10})$, and its corresponding Delannoy paths. To the right, the edges on which possible paths can occur for this domain. This vertices of the possible paths lie in the lattice $\mathbb{Z}^2$ after the transformation described above.

Determinants

As done in [8], from the bijection in Proposition 3.3.1, we can use the Lindström–Gessel–Viennot Lemma [11] [18] to write the number of Case 1 sequences when $w_{2t+1} = +$, for all t, as a determinant of a matrix whose entries are in D.

Corollary 3.3.3. *The number of Case 1 sequences for $\mu = (\mu_1, \ldots, \mu_n)$ and w such that $w_{2t+1} = +$ for all t is given by* $\det(A)$ *where*

$$A_{i,j} = D(\mu_{n-j+1} + j - W_i - 1, i - 1)$$

and $W_i = \#\{w_{2t} = + \mid t > n - i\}$.

Note that since we are taking east, south, and southeast steps in our Delannoy paths instead of the north, east, and northeast steps in Definition 3.1.3, the number of paths from (x_1, y_1) to (x_2, y_2) is given by $D(x_2 - x_1, y_1 - y_2)$.

For Case 2 sequences, we note that a path from $(0, 0)$ to (x, y) without ending in an east step is counted by $H(x, y-1)$ (see Definition 3.1.5). Then similarly for Case 2 sequences we have

Corollary 3.3.4. *The number of Case 2 sequences for $\mu = (\mu_1, \ldots, \mu_n)$ and w such that $w_{2t+1} = +$ for all t is given by* $\det(A)$ *where*

$$A_{i,j} = H(\mu_{n-j+1} + j - W_i - 1, i - 1)$$

and $W_i = \#\{w_{2t} = + \mid t > n - i\}$.

More non-intersecting paths

In this section we will explore other ways of assigning paths to dominoes in a domino tiling of a domain, and the resulting matrix whose determinant enumerates the number of domino tilings on said domain. We will only consider generalized Aztec triangles resulting from partitions of the form $(k, k-1, \ldots, 1, 0^{n-k})$ with positive w. These are exactly the generalized Aztec triangles for which we have a product formula in Theorem 3.4.3.

First we consider associating dominoes in a domino tiling to paths via Figure 3.18. We can use an argument similar to our second proof of Proposition 3.3.1 to see that the resulting non-intersecting paths must start from light squares on the northwest boundary of our domain and end in the dark squares along the southeast boundary of our domain, as illustrated in Figure 3.19.

We can use these paths to construct another matrix whose determinant will give us the number of tilings on our generalized Aztec triangle. Similar to before, we will consider a change of coordinates so that it will be easier to express the coordinates of the starting and ending points of our paths. In this case, we rotate by $-\frac{3\pi}{4}$, dilate by $\sqrt{2}$, and translate so that the origin is at the midpoint of the north edge of the north-most light square. See Figure 3.19 for the origin after our transformation. For the remainder of this section we will use north, south, east, west to refer to directions before our change of coordinates.

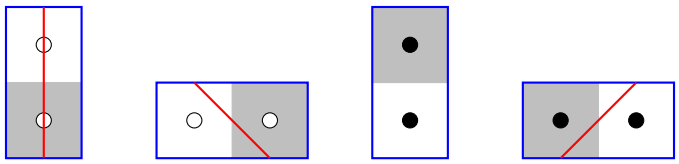

Figure 3.18: Another way to assign paths to each domino in a domino tiling, which results in the determinants in Proposition 3.3.5.

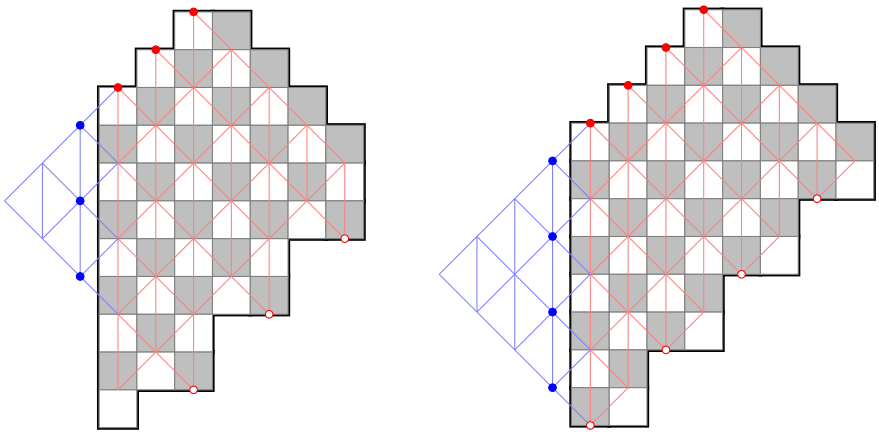

Figure 3.19: The grid on which paths in this new bijection can take. On the left we have the Case 1 domain for the partition $(3, 2, 1, 0, 0)$ and on the right the Case 2 domain for the partition $(4, 3, 2, 1)$. Filled red points denote the starts of our paths, unfilled red points denote the ends of our paths, and blue points are additional trivial paths we add to compute our determinants. The north-most filled red point is our origin after our change of coordinates.

Proposition 3.3.5. *The number of Case 1 sequences for a partition* $\mu = (k, \ldots, 1, 0^{n-k})$ *with* $w = (+^{2n-1})$ *is given by the determinant of a* $2k \times 2k$ *matrix* B *where*

$$B_{i,j} = \begin{cases} H(2j-i, n-1) & i,j \leq k \\ H(2j-i, n-i+k-2) & i > k, j \leq k \\ D(j-i, j-k-1) & i \leq k, j > k \\ D(j-i, j-i) & i,j > k \end{cases}$$

The number of Case 2 sequences for a partition $\mu = (k, k-1, \ldots, 1, 0^{n-k})$ *with* $w = (+^{2n})$ *is*

given by the determinant of a $2k \times 2k$ matrix B where

$$B_{i,j} = \begin{cases} D(2j-i, n-1) & i,j \leq k \\ D(2j-i, n-i+k-2) & i > k, j \leq k \\ D(j-i, j-k-1) & i \leq k, j > k \\ D(j-i, j-i) & i,j > k \end{cases}$$

Proof. Consider first Case 1. Let us extend our domain to the left as in the blue grid in Figure 3.19 to ensure that our paths are H paths as defined in Definition 3.1.5 (note that the last diagonal of our domain being an incomplete diagonal of dark squares guarantees that our paths end as in Definition 3.1.5). Then as noted above we can follow the second proof of Proposition 3.3.1 and find the starting points and ending points of our paths to construct a determinant that enumerates our non-intersecting paths. We get k starting points $(i-1, 0)$ and k ending points $(2i-1, n-1)$ for $i = 1, \ldots, k$.

Now to prevent our paths from exiting our domain, we can add k trivial paths at the points in blue pictured in Figure 3.19. This adds k more starting and ending points at $(k+i-1, i-1)$ for $i = 1, \ldots, k$. Noting that paths which end at these k additional ending points are Delannoy paths, we have our proposition for Case 1.

Case 2 follows similarly, noting that instead of H paths now our paths are all Delannoy paths (again see Figure 3.19). Recall also from Definition 3.1.5 that $H(i,j)$ counts the number of H paths from $(0,0)$ to $(i, j+1)$. □

Remark 3.3.6. If we wish to express this matrix without the added trivial paths, consider our $2k \times 2k$ matrix as four $k \times k$ block matrices $\begin{bmatrix} A_1 & A_2 \\ A_3 & A_4 \end{bmatrix}$. Then the matrix that enumerates paths that lie strictly in our domain (without the trivial paths) is given by $B_1 - B_2 B_4^{-1} B_3$. For example the number of Case 1 sequences for the partition $(3,2,1,0,0)$ and the number of Case 2 sequences for the partition $(4,3,2,1)$ from Figure 3.19 are given by the determinants, respectively

$$\begin{vmatrix} 10 & 170 & 1002 & 1 & 9 & 61 \\ 1 & 50 & 450 & 1 & 7 & 41 \\ 0 & 10 & 170 & 1 & 5 & 25 \\ 0 & 1 & 50 & 1 & 3 & 13 \\ 0 & 0 & 8 & 0 & 1 & 3 \\ 0 & 0 & 1 & 0 & 0 & 1 \end{vmatrix} = \begin{vmatrix} 10 & 169 & 874 \\ 1 & 49 & 352 \\ 0 & 9 & 98 \end{vmatrix} = 7644$$

$$\begin{vmatrix} 9 & 129 & 681 & 2241 & 1 & 11 & 85 & 575 \\ 1 & 41 & 321 & 1289 & 1 & 9 & 61 & 377 \\ 0 & 9 & 129 & 681 & 1 & 7 & 41 & 231 \\ 0 & 1 & 41 & 321 & 1 & 5 & 25 & 129 \\ 0 & 0 & 9 & 129 & 1 & 3 & 13 & 63 \\ 0 & 0 & 1 & 25 & 0 & 1 & 3 & 13 \\ 0 & 0 & 0 & 5 & 0 & 0 & 1 & 3 \\ 0 & 0 & 0 & 1 & 0 & 0 & 0 & 1 \end{vmatrix} = \begin{vmatrix} 9 & 129 & 664 & 1408 \\ 1 & 41 & 306 & 714 \\ 0 & 9 & 116 & 304 \\ 0 & 1 & 30 & 90 \end{vmatrix} = 32032$$

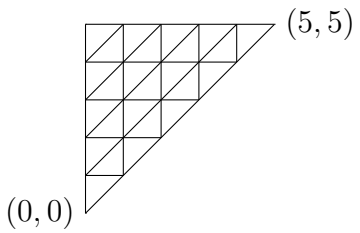

Figure 3.20: The paths that the 5th Schröder number counts.

Definition 3.3.7. The *nth Schröder number* is the number of paths from $(0,0)$ to (n,n) using east, north, and northeast steps that do not go below the line $y = x$.

See Figure 3.20 for the paths that the 5th Schröder number counts. With this definition we can now observe another special case of our generalized Aztec triangles.

Proposition 3.3.8. *Let A_n^1 be the matrix from Corollary 3.3.3 for the partition (1^n) and A_n^2 the matrix from Corollary 3.3.4 for the same partition, so that*

$$A^l_{n,(i,j)} = H_l(i - j + 1, i - 1)$$

Then

$$|A^1_{n+1}| = |A^2_n| = S_n$$

where S_n is the nth Schröder number.

Proof. Though the partition (1^n) is not addressed in Proposition 3.3.5, we can consider the paths we get for the domain corresponding to this partition. Recall that these paths begin on north-most light squares and end at south-most dark squares. Hence it follows that there is a single path beginning at $(0,0)$ and ending at (n,n) as pictured in Figure 3.21 (we still use the same transformation as in Proposition 3.3.5). However for Case 1, the path is fixed from $(n-1, n-1)$ to (n,n). Finally, since our domain requires that our paths do not go below $y = x$, we see that they are exactly Schröder paths and our proposition is proved. □

Now let us associate dominoes to paths via Figure 3.22. Again we will use a change of coordinates to describe these paths – this time rotate by $\frac{-3\pi}{4}$, dilate by $\sqrt{2}$, and finally translate so that our origin is at the midpoint of the north edge of the east-most dark square (north-most if there are multiple). Again see the red points in Figure 3.23 for where our origin is located.

We follow the previous proof for Proposition 3.3.5 referencing Figure 3.23. This time we have n Delannoy paths beginning at $(0, i-1)$ for $i = 1, \ldots, n$ and ending at $(2i-2, n-1)$ for $i = 1, \ldots, k$ and $(i+k-1, n-1)$ for $i = k+1, \ldots, n$. As in Proposition 3.3.5 we add in some trivial paths which are pictured in blue in Figure 3.23, which are at $(i+k, i-1)$ for

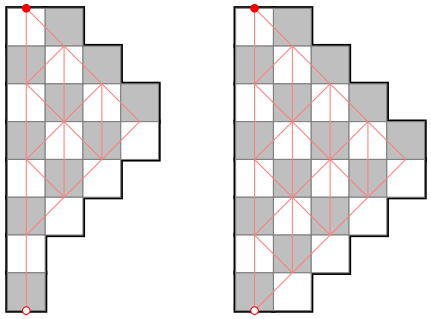

Figure 3.21: The Case 1 and Case 2 domains, respectively, for the partition $(1,1,1,1)$. Assigning paths using Figure 3.18 gives the red grid pictured, which is a single Schröder path.

$i = 1, \ldots, n-1$. (Note that for Case 1, the n starting point is also a trivial path). Finally observing that Case 1 gives rise to Delannoy paths and Case 2 gives rise to H paths, we have the following proposition:

Proposition 3.3.9. *The number of Case 1 sequences for a partition $\mu = (k, \ldots, 1, 0^{n-k})$ with $w = (+^{2n-1})$ is given by the determinant of a $(2n-1) \times (2n-1)$ matrix C where*

$$C_{i,j} = \begin{cases} D(2j-2, n-i) & i \leq n, j \leq k \\ D(2j-i+n-k-2, 2n-i) & i > n, j \leq k \\ D(j+k-1, n-i) & i \leq n, k < j \leq n \\ D(j-i+n-1, 2n-i) & i > n, k < j \leq n \\ D(j+k-n, j-i-n) & i \leq n, j > n \\ D(j-i, j-i) & i, j > n \end{cases}$$

The number of Case 2 sequences for a partition $\mu = (k, k-1, \ldots, 1, 0^{n-k})$ with $w = (+^{2n})$ is given by the determinant of a $(2n-1) \times (2n-1)$ matrix C where

$$C_{i,j} = \begin{cases} H(2j-2, n-i) & i \leq n, j \leq k \\ H(2j-i+n-k-2, 2n-i) & i > n, j \leq k \\ H(j+k-1, n-i) & i \leq n, k < j \leq n \\ H(j-i+n-1, 2n-i) & i > n, k < j \leq n \\ D(j+k-n, j-i-n) & i \leq n, j > n \\ D(j-i, j-i) & i, j > n \end{cases}$$

Again, we can apply Remark 3.3.6 to find the matrix without the additional trivial paths.

Our final way to associate dominoes to paths is given in Figure 3.24. Our change of coordinates for these paths is given by first reflection over the y-axis, rotation by $\frac{-\pi}{4}$, dilation

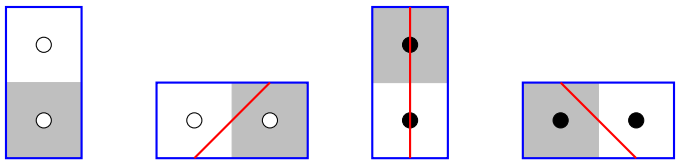

Figure 3.22: A third way to assign paths to each domino in a domino tiling, which results in the determinants in Proposition 3.3.9.

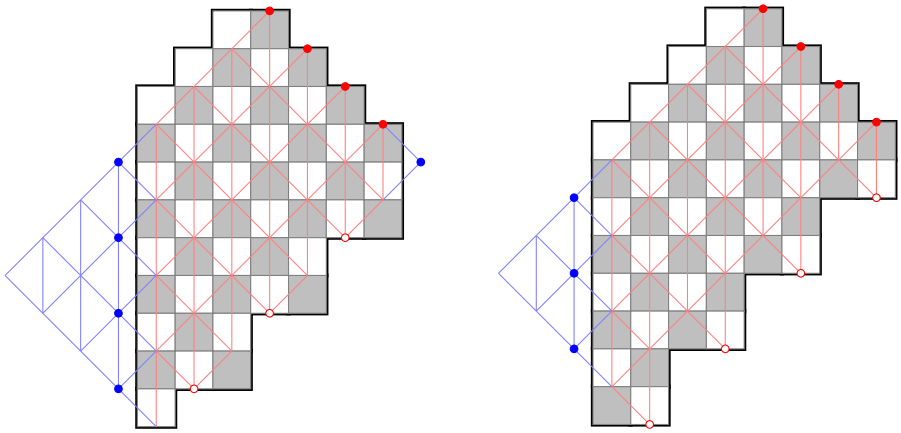

Figure 3.23: The grid on which paths in Proposition 3.3.9 can take. On the left we have the Case 1 domain for the partition $(3, 2, 1, 0, 0)$ and on the right the Case 2 domain for the partition $(4, 3, 2, 1)$. Filled red points denote the starts of our paths, unfilled red points denote the ends of our paths, and blue points are additional trivial paths we add to compute our determinants. The north-most filled red point is our origin after our change of coordinates.

by $\sqrt{2}$, and translation so that the origin is at the midpoint of the west edge of the west-most square of the first diagonal. Figure 3.3 identifies the origin for two such transformations.

As before we find the starting and ending points of these paths. For starting points we have $(0, k-i)$ for $i = 1, \ldots, k$ and $(i, -i)$ for $i = 1, \ldots, n-1$. For ending points we have $(i, k-1)$ for $i = 1, \ldots, n-1$ which are Delannoy paths in both Case 1 and Case 2. For Case 1 we also have $(n-1, k-2i+1)$ for $i = 1, \ldots, k$ which are are H paths after being reflected over the line $y = x$. For Case 2 we have instead $(n, k-2i+1)$ for $i = 1, \ldots, k$ which are Delannoy paths for $i \geq 2$ and an H path for $i = 1$. Also in Case 2 when $n > k$ we have an additional starting point $(n, -n)$ and ending point $(n-1, -k-1)$ which is a Delannoy path.

Proposition 3.3.10. *The number of Case 1 sequences for a partition* $\mu = (k, \ldots, 1, 0^{n-k})$

with $w = (+^{2n-1})$ *is given by the determinant of a* $(n+k-1) \times (n+k-1)$ *matrix* D *where*

$$D_{i,j} = \begin{cases} H(j, i-1) & i \leq k, j < n \\ H(j-i+k, i-1) & i > k, j < n \\ H(2n-2j+i-1, n-1) & i \leq k, j \geq n \\ H(2n-2j+i-1, n+k-i-1) & i > k, j \geq n \end{cases}$$

The number of Case 2 sequences for a partition $\mu = (k, \ldots, 1)$ *with* $w = (+^{2n})$ *is given by the determinant of a* $(n+k-1) \times (n+k-1)$ *matrix* D *where*

$$D_{i,j} = \begin{cases} H(j, i-1) & i \leq k, j < n \\ H(j-i+k, i-1) & i > k, j < n \\ H(n, i-1) & i \leq k, j = n \\ H(n+k-i, i-1) & i > k, j = n \\ D(n, 2n-2j+i-1) & i \leq k, j > n \\ D(n+k-i, 2n-2j+i-1) & i > k, j > n \end{cases}$$

The number of Case 2 sequences for a partition $\mu = (k, k-1, \ldots, 1, 0^{n-k})$ *where* $n > k$ *with* $w = (+^{2n+1})$ *is given by the determinant of a* $(n+k) \times (n+k)$ *matrix* D *where*

$$D_{i,j} = \begin{cases} H(j, i-1) & i \leq k, j < n \\ H(j-i+k, i-1) & i > k, j < n \\ H(n, i-1) & i \leq k, j = n \\ H(n+k-i, i-1) & i > k, j = n \\ D(n, 2n-2j+i-1) & i \leq k, j > n \\ D(n+k-i, 2n-2j+i-1) & i > k, j > n \end{cases}$$

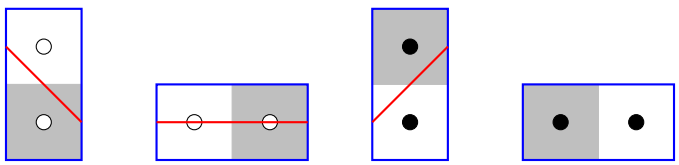

Figure 3.24: A fourth way to assign paths to each domino in a domino tiling, which results in the determinants in Proposition 3.3.10.

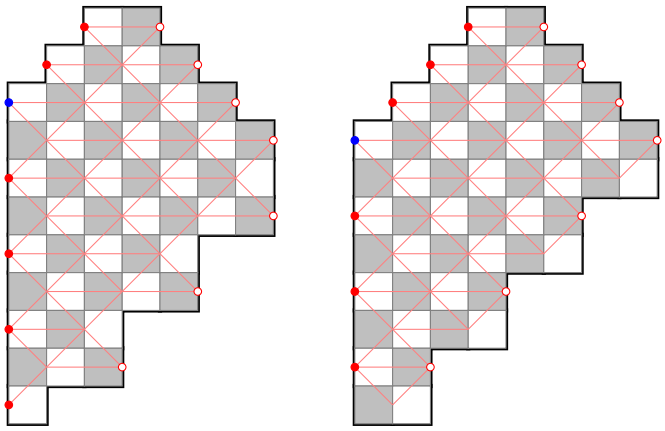

Figure 3.25: The grid on which paths in Proposition 3.3.10 can take. On the left we have the Case 1 domain for the partition $(3, 2, 1, 0, 0)$ and on the right the Case 2 domain for the partition $(4, 3, 2, 1)$. Filled points denote the starts of our paths and unfilled points denote the ends of our paths, The blue point is our origin after our change of coordinates.

3.4 Positive w

Tableaux

Here we will identify another combinatorial object that is in bijection with Case 1 and 2 sequences for the case when w is positive.

Proposition 3.4.1. *When $w_t = +$ for all t, Case 1 sequences for any μ are in bijection with super symplectic tableaux of shape μ with entries $1 < \overline{1} < \cdots < n$.*

Proof. The bijection is established by considering putting entries i in the cells corresponding to $\lambda_{2i-1}/\lambda_{2i-2}$, and entries $\bar{\imath}$ in the cells corresponding to $\lambda_{2i}/\lambda_{2i-1}$. The restriction on the number of nonzero parts in any λ_i guarantees our symplectic condition. Conversely, given such a tableau we can recover λ_{2i} by taking the cells of the tableau with entries at most $\bar{\imath}$, and we can recover λ_{2i+1} by taking the cells of the tableau with entries at most $i + 1$. See Figure 3.26. □

This proof also applies to Case 2 sequences:

Proposition 3.4.2. *When $w_t = +$ for all t, Case 2 sequences for any μ are in bijection with super symplectic tableaux of shape μ with entries $1 < \overline{1} < \cdots < n < \overline{n}$.*

Given a super symplectic tableau of shape $\mu = (\mu_1, \ldots, \mu_n)$, the unbarred entries in row l give the locations of the east steps of path $n + l - i$ (the lth north-most path), and the barred entries give the locations of the southeast steps. Specifically if row l of the super

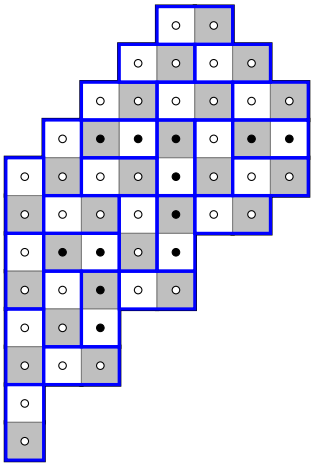

1	1	$\overline{1}$	3	$\overline{3}$
2	$\overline{2}$	3		
3	3			
4				

Figure 3.26: A domino tiling on the generalized Aztec triangle for $\mu = (5, 3, 2, 1)$, and the corresponding super symplectic tableau.

symplectic tableau contains the unbarred entry i exactly m times, then path $n + 1 - i$ has exactly m east steps between diagonals $2i - 2$ and $2i - 1$. If row l contains the barred entry $\bar{\imath}$, then path $n + 1 - i$ has a southeast step that begins before diagonal $2i - 1$ and ends after diagonal $2i$. With the addition of south steps there is a unique way of realizing this path, which completes the bijection from super symplectic tableaux to non-intersecting Delannoy paths.

Product formulas

Theorem 3.4.3. *When $\mu = (k, k-1, \ldots, 1, 0^{n-k})$ and $w = (+^{2n-1})$, the number of Case 1 sequences is given by*

$$\prod_{j\geq 0}\left(\prod_{i=-2k+4j+1}^{-k+2j}(2n+i)\prod_{i=k-2j}^{2k-4j-2}(2n+i)\right)\Bigg/\prod_{j=1}^{k-1}(2j+1)^{k-j}$$

When $\mu = (k, k-1, \ldots, 1, 0^{n-k})$ and $w = (+^{2n})$, the number of Case 2 sequences is given by

$$\prod_{j\geq 0}\left(\prod_{i=-2k+4j+1}^{-k+2j}(2n+i+1)\prod_{i=k-2j}^{2k-4j-2}(2n+i+1)\right)\Bigg/\prod_{j=1}^{k-1}(2j+1)^{k-j}$$

More generally, the number of sequences $\lambda^{(0)}, \ldots, \lambda^{(\ell-1)}$ as defined in Definition 3.1.1 (Case 1 if $\ell - 1$ is odd and Case 2 if $\ell - 1$ is odd) is given by

$$\prod_{j\geq 0}\left(\prod_{i=-2k+4j+1}^{-k+2j}(\ell+i)\prod_{i=k-2j}^{2k-4j-2}(\ell+i)\right)\Bigg/\prod_{j=1}^{k-1}(2j+1)^{k-j}$$

The proof for Theorem 3.4.3 uses the determinant for Case 1 found in Corollary 3.3.3 to prove the first product formula. From this, the formula for Case 2 is a consequence of Theorem 3.4.4 below (and then the third formula immediately follows). The full details of the proof can be found in Sections 4 and 5 of [6]. For the remainder of this section, we will observe some properties and consequences regarding this formula.

We observe that Theorem 3.4.3 for Case 2 sequences can be obtained from that of Case 1 sequences by taking values of n in $\frac{1}{2}+\mathbb{Z}$. In fact, we can show that a similar relation holds when computing computing determinants from Corollaries 3.3.3 and 3.3.4. In this case of $\mu = (k, \ldots, 1, 0^{n-k})$ and $w = (+^{2n-1})$, Corollary 3.3.3 gives us the $n \times n$ matrix

$$A^1_{i,j} = D(\mu_{n-j+1} + j - i, i - 1)$$

whose determinant is determined by its bottom right $k \times k$ entries

$$M^1_{i,j} = D(2j - i, i + n - k - 1)$$

Similarly in this case Corollary 3.3.4 gives us the $n \times n$ matrix

$$A^2_{i,j} = H(\mu_{n-j+1} + j - i, i - 1)$$

again whose determinant is determined by the bottom right $k \times k$ entries

$$M^2_{i,j} = H(2j - i, i + n - k - 1)$$

In particular M^1 and M^2 depend only on k, n so we can define $M^1(k, n)$ and $M^2(k, n)$ to be the $k \times k$ matrices above.

Theorem 3.4.4. *For $n, k \in \mathbb{Z}_{\geq 0}$*

$$\det(M^1(k, n + \tfrac{1}{2})) = \det(M^2(k, n))$$

The entries of M^1 are all of the form $D(i, j)$ for some $i, j \in \mathbb{Z}$. Let us redefine $D(i, j)$ using one of the identities in Proposition 3.1.6:

$$D(i, j) = \sum_{m=0}^{i}\binom{i}{m}\binom{j}{m}2^m$$

where now we allow any $j \in \mathbb{R}$. In particular here our binomial coefficients $\binom{j}{m}$ are defined for $j \in \mathbb{R}$ by

$$\binom{j}{m} = \frac{j(j-1)(j-2)\cdots(j-m+1)}{m!}$$

and $\binom{j}{m} = 0$ if $m < 0$.

Proof of Theorem 3.4.4. Our claim follows from Proposition 3.4.6 below: that for $i, j \in \mathbb{Z}_{\geq -1}$

$$D(i, j+\tfrac{1}{2}) = \sum_{l=0}^{\lceil i/2 \rceil} (-1)^l \binom{-\frac{1}{2}}{l} H(i-2l, j)$$

Then our definitions of M^1 and $M^2 2$ then give us that $M^1(k, n+\frac{1}{2})$ can be obtained by column operations $M^2(k, n)$ hence proving their determinants are equal. □

Lemma 3.4.5. *For all $i \in \mathbb{Z}, j \in \mathbb{R}$ we have*

$$D(i, j) = D(i-1, j) + D(i-1, j-1) + D(i, j-1)$$

$D(i, j)$ is defined by

$$D(i, j) = \sum_{m=0}^{i} \binom{i}{m}\binom{j}{m} 2^m$$

Proof. This is part of the Remark 3.1.4, but as we cannot use our combinatorial definition

of $D(i,j)$ we compute directly

$$\begin{aligned}
D(i,j) &= \sum_{m=0}^{i} \binom{i}{m}\binom{j}{m}2^m \\
&= \sum_{m=0}^{i-1} \binom{i-1}{m}\binom{j}{m}2^m + \sum_{m=1}^{i} \binom{i-1}{m-1}\binom{j}{m}2^m \\
&= D(i-1,j) + \sum_{m=1}^{i} \binom{i-1}{m-1}\binom{j-1}{m}2^m + \sum_{m=1}^{i} \binom{i-1}{m-1}\binom{j-1}{m-1}2^m \\
&= D(i-1,j) + D(i-1,j-1) + \sum_{m=1}^{i} \binom{i-1}{m-1}\binom{j-1}{m}2^m \\
&\quad + \sum_{m=1}^{i} \binom{i-1}{m-1}\binom{j-1}{m-1}2^{m-1} \\
&= D(i-1,j) + D(i-1,j-1) + \sum_{m=1}^{i} \binom{i-1}{m-1}\binom{j-1}{m}2^m \\
&\quad + \sum_{m=0}^{i-1} \binom{i-1}{m}\binom{j-1}{m}2^m \\
&= D(i-1,j) + D(i-1,j-1) + \sum_{m=0}^{i} \binom{i}{m}\binom{j-1}{m}2^m \\
&= D(i-1,j) + D(i-1,j-1) + H(i,j-1)
\end{aligned}$$

□

Proposition 3.4.6. *For $i,j \in \mathbb{Z}_{\geq -1}$*

$$D(i,j+\tfrac{1}{2}) = \sum_{l=0}^{\lceil i/2 \rceil} (-1)^l \binom{-\frac{1}{2}}{l} H(i-2l,j)$$

where $D(i,j)$ is defined by

$$D(i,j) = \sum_{m=0}^{i} \binom{i}{m}\binom{j}{m}2^m$$

Proof. We will induct on j. For our inductive step we will prove our statement

$$D(i,j+\tfrac{1}{2}) = \sum_{l=0}^{\lceil i/2 \rceil} (-1)^l \binom{-\frac{1}{2}}{l} H(i-2l,j)$$

for any $i \geq -1$ and some fixed $j \geq 0$ given that it holds for $j-1$. For this we will additionally induct on i. Again we begin with the inductive step. Using Lemma 3.4.5 along with the

identity $H(i,j) = H(i-1,j) + H(i,j-1) + H(i-1,j-1)$ from Proposition 3.1.6 to see that for $i, j \geq 0$

$$\begin{aligned} D(i, j+\tfrac{1}{2}) &= D(i-1, j+\tfrac{1}{2}) + D(i-1, j-\tfrac{1}{2}) + H(i, j-\tfrac{1}{2}) \\ &= \sum_{l=0}^{\lceil (i-1)/2 \rceil} (-1)^l \binom{-\frac{1}{2}}{l} H(i-1-2l, j) \\ &\quad + \sum_{l=0}^{\lceil (i-1)/2 \rceil} (-1)^l \binom{-\frac{1}{2}}{l} H(i-1-2l, j-1) \\ &\quad + \sum_{l=0}^{\lceil i/2 \rceil} (-1)^l \binom{-\frac{1}{2}}{l} H(i-2l, j-1) \\ &= \sum_{l=0}^{\lceil i/2 \rceil} (-1)^l \binom{-\frac{1}{2}}{l} H(i-2l, j) \end{aligned}$$

noting that $H(i,j) = 0$ for $i < 0$ and all j. Now for the base case $i = -1$ we have

$$D(-1, j+\tfrac{1}{2}) = 0 = H(-1, j)$$

for all j, as desired.

It remains to be seen that the base case $j = -1$ holds, that is

$$D(i, -\tfrac{1}{2}) = \sum_{l=0}^{\lceil i/2 \rceil} (-1)^l \binom{-\frac{1}{2}}{l} H(i-2l, -1)$$

for all $i \geq 0$. Now

$$H(i,-1) = \begin{cases} 1 & i = 0 \\ 0 & \text{else} \end{cases}$$

so we wish to show

$$D(i, -\tfrac{1}{2}) = \sum_{m=0}^{i} \binom{i}{m} \binom{-\frac{1}{2}}{m} 2^m = \begin{cases} 0 & i \text{ odd} \\ \left| \binom{-1/2}{i/2} \right| & i \text{ even} \end{cases}$$

Now we note that the terms of the summation above satisfy

$$\frac{\binom{i}{m+1}\binom{-\frac{1}{2}}{m+1} 2^{m+1}}{\binom{i}{m}\binom{-\frac{1}{2}}{m} 2^m} = \frac{(m-i)(m+\frac{1}{2})}{(m+1)^2} \cdot 2$$

and so by definition it is the hypergeometric series [20]

$$\sum_{m=0}^{i} \binom{i}{m}\binom{-\frac{1}{2}}{m}2^m = {}_2F_1\left[\begin{matrix}\frac{1}{2}, & -i \\ & 1\end{matrix}; 2\right]$$

Using Mathematica we also find that it evaluates to

$$\sum_{m=0}^{i} \binom{i}{m}\binom{-\frac{1}{2}}{m}2^m = \frac{\left(1+(-1)^i\right)\Gamma\left(\frac{i+1}{2}\right)}{\sqrt{\pi}i\Gamma\left(\frac{i}{2}\right)}$$

for $i > 0$. When i is odd the right hand side is equal to 0 as desired. Otherwise when i is even we can induct on i. Beginning with $i = 2$ (it is easy to check directly that $i = 0$ holds) we find that

$$\frac{\left(1+(-1)^2\right)\Gamma\left(\frac{3}{2}\right)}{\sqrt{\pi}2\Gamma\left(1\right)} = \frac{1}{2} = \left|\binom{-\frac{1}{2}}{l}\right|$$

And when $i = 2(t+1)$ we have by inductive hypothesis

$$\frac{2\Gamma\left(\frac{2t+3}{2}\right)}{\sqrt{\pi}2(t+1)\Gamma\left(t+1\right)} = \frac{(2t+1)\Gamma\left(\frac{2t+1}{2}\right)}{\sqrt{\pi}2(t+1)t\Gamma(t)} = \frac{2t+1}{2(t+1)}\cdot\left|\binom{-\frac{1}{2}}{t}\right| = \left|\binom{-\frac{1}{2}}{t+1}\right|$$

This concludes the base case of our induction on j and we have our result. □

Theorem 3.4.7. *The number of Case 1 sequences for the partition $\mu = (k+1, k, \ldots, 1)$ with $w = (+^{2k+1})$ is equal to the number of Case 2 sequences for the partition $\mu = (k, k-1, \ldots, 1, 0)$ with $w = (+^{2k+2})$.*

Proof. Using our formula from Theorem 3.4.3 we wish to show that

$$\prod_{j=0}^{\lfloor\frac{k}{2}\rfloor}\prod_{i=-2k+4j-1}^{-k+2j-1}(2k+i+2)\cdot\prod_{j=0}^{\lfloor\frac{k-1}{2}\rfloor}\prod_{i=k-2j+1}^{2k-4j}(2k+i+2)\Bigg/\prod_{j=1}^{k}(2j+1)^{k+1-j}$$
$$=\prod_{j=0}^{\lfloor\frac{k-1}{2}\rfloor}\prod_{i=-2k+4j+1}^{-k+2j}(2k+i+3)\cdot\prod_{j=0}^{\lfloor\frac{k-2}{2}\rfloor}\prod_{i=k-2j+2}^{2k-4j}(2k+i+3)\Bigg/\prod_{j=1}^{k-1}(2j+1)^{k-j}$$

This is done in Computation A.0.1. □

Figure 3.27 shows two generalized Aztec triangles that Theorem 3.4.7 state must have an equal number of domino tilings. We also present an alternative proof for Theorem 3.4.7 by using our determinants from Corollaries 3.3.3 and 3.3.4.

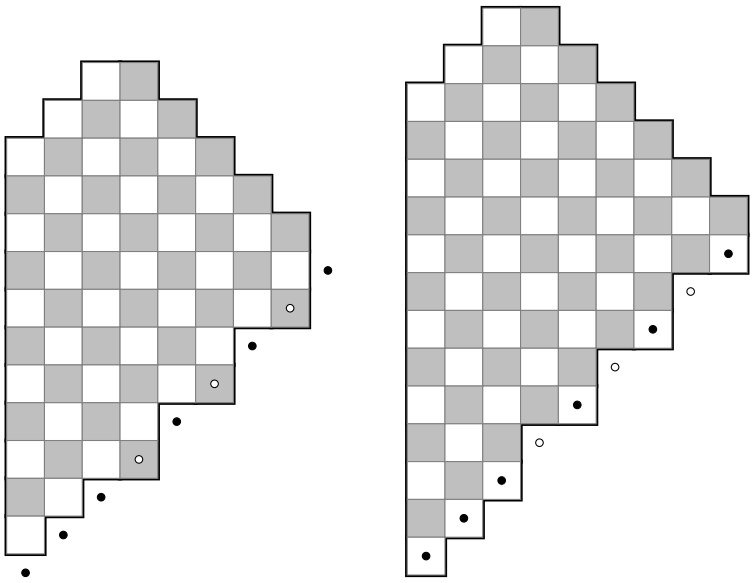

Figure 3.27: By Theorem 3.4.7, these two generalized Aztec triangles have the same number of domino tilings.

Alternate proof of Theorem 3.4.7. Let A be the matrix from Corollary 3.3.3 for the partition $(k+1, k, \ldots, 1)$ and let B be the matrix from Corollary 3.3.4 for the partition $(k, k-1, \ldots, 1, 0)$. Then

$$A_{i,j} = D(2j-i, i-1) \text{ and } B_{i,j} = H(2j-i-1, i-1)$$

We claim that

$$H(i,j) = \sum_{k=0}^{j} (-1)^{j-k} (D(i+1+j-k, k) + D(i-1+j+k, k))$$

whence we have

$$\begin{aligned} H(2j-i-1, i-1) &= \sum_{k=0}^{i-1} (-1)^{i-1-k} (D(2j-k, k) + D(2j-3-k, k)) \\ &= \sum_{k=1}^{i} (-1)^{i-k} (D(2j-k, k-1) + D(2j-k-2, k-1)) \\ B_{i,j} &= \sum_{k=1}^{i} (-1)^{i-k} (A_{k,j} + A_{i,j-1}) \end{aligned}$$

And it would follow that $\det(A) = \det(B)$ since B is obtained from a series of row and column operations on A. Now let us prove our claim by inducting on j. We wish to show

that

$$\begin{aligned} H(i,j) = (D(i+1,j) + D(i-1,j)) - (D(i+2,j-1) + D(i,j-1)) + \cdots \\ \pm (D(i+1+j,0) + D(i-1+j,0)) \end{aligned}$$

Using some identities from Proposition 3.1.6 we see that

$$\begin{aligned} H(i,j) &= D(i,j) + D(i-1,j) \\ &= D(i+1,j) - D(i+1,j-1) - D(i,j-1) + D(i-1,j) \\ &= (D(i+1,j) + D(i-1,j)) - H(i+1,j-1) \end{aligned}$$

thus proving both our claim and proposition. □

Remark 3.4.8. Finally let us observe that this formula is actually a generalization of Di Francesco's conjectured formula [8]:

$$F(n) := 2^{n(n-1)/2} \prod_{i=0}^{n-1} \frac{(4i+2)!}{(n+2i+1)!}$$

Indeed when $\mu = (n, n-1, \ldots, 1)$, Conjecture 3.4.3 gives us that the number of Case 1 sequences is equal to

$$\begin{aligned} G(n) &:= \prod_{j \geq 0} \left(\prod_{i=-2n+4j+1}^{-n+2j} (2n+i) \prod_{i=n-2j}^{2n-4j-2} (2n+i) \right) \Bigg/ \prod_{j=1}^{n-1} (2j+1)^{n-j} \\ &= \prod_{j \geq 0} \left(\prod_{i=4j+1}^{n+2j} i \prod_{i=3n-2j}^{4n-4j-2} i \right) \Bigg/ \prod_{j=1}^{n-1} (2j+1)^{n-j} \end{aligned}$$

Now we compute for $n \geq 1$

$$\begin{aligned} \frac{F(n+1)}{F(n)} &= 2^n \cdot \frac{(4n+2)!}{(3n+2)!} \prod_{i=0}^{n-1} \frac{(n+2i+1)!}{(n+2i+2)!} = 2^n \cdot \frac{(4n+2)!}{(3n+2)!} \prod_{i=0}^{n-1} \frac{1}{n+2i+2} \\ &= \frac{2^n (4n+2)! n!!}{(3n+2)! (3n)!!} \end{aligned}$$

where $n!!$ is the product of all integers from 1 to n with the same parity as n.

A lengthier computation done in Computation A.0.2 shows that $\frac{F(n+1)}{F(n)} = \frac{G(n+1)}{G(n)}$ for all $n \geq 1$. Then along with the fact that $F(1) = G(1) = 1$, we see that $F(n) = G(n)$ for all $n \geq 1$. Hence indeed, Di Francesco's conjectured formula [8, Conj. 8.1] results as a special case from Theorem 3.4.3.

3.5 Conclusion

The original motivation [8] for studying domino tilings of Aztec triangles was to obtain a combinatorial object for which there exists a bijection to configurations of the 20V model on trapezoidal domains $\mathcal{T}_n$. We now have a generalized Aztec triangle that depends on parameters μ, w, and m as well as being either Case 1 or Case 2. However since there was no explicit bijection from domino tilings of Aztec triangles to configurations of the 20V model, it is unclear what the relation is from generalized Aztec triangles to 20V model configurations. The relation is unknown even when $\mu = (k, k-1, \ldots, 1, 0^{n-k})$ and w is positive as in the case of Theorem 3.4.3 where we have a product formula for enumerating its domino tilings.

One way to relate domino tilings of generalized Aztec triangles back to configurations of the 20V model is suggested by Di Francesco [8]. He additionally conjectures that the number domino tilings of the Aztec triangle with the first $k-1$ rows (consistent with Di Francesco's definition of $\mathcal{T}_{n,n-k}$) removed is equal to 20V model configurations on particular pentagonal domains. In fact, he proves (see Section 7) this conjecture for $k = 2, 3$ through combinatorial means (with $k = 1$ being the entire Aztec triangle). Larger values of k remain open, and combinatorial proofs in these cases seem much more complicated.

We can think of $\mathcal{T}_{n,n-k}$ – the Aztec triangle with $k-1$ rows removed – as an Aztec triangle where the first $k-1$ rows are forced to have horizontal dominoes. Then in terms of the sequences of partitions, domino tilings of $\mathcal{T}_{n,n-k}$ correspond to sequences as described in Definition 3.1.1 with $\mu = (n, n-1, \ldots, 1)$ and the additional condition that $\lambda_j^{(i)} \leq n - (k-1) + \lfloor \frac{i}{2} \rfloor$ for all i, j. So while we can also interpret domino tilings of $\mathcal{T}_{n,n-k}$ as sequences of partitions, they are not directly addressed here.

Furthermore we can also reformulate this in terms of tableaux: domino tilings of $\mathcal{T}_{n,n-k}$ correspond to fillings of the Young diagram of shape $(n, n-1, \ldots, 1)$ with entries $1 < \overline{1} < 2 < \overline{2} < \cdots < n$ subject to the conditions in Proposition 1.5 and also additionally that the entries i and $\overline{i-1}$ do not appear past the $(n-k+i)$th column.

Finally it is unknown which other classes of generalized Aztec triangles can be explicitly enumerated. Based on experimental data computed from the determinants in Corollaries 3.3.3 and 3.3.4, it seems that other choices μ, w, and m do not permit a simple product formula as in Theorem 3.4.3. It is very possible that some generalization of Schur functions could be used here – see the usage of Schur functions in Section 3.13. This question of enumeration could also involve construction of an even more general Aztec triangle, for example to include the aforementioned domains $\mathcal{T}_n, n-k$. Still, in this case it seems unlikely that a simple product formula would suffice to enumerate its domino tilings.

Bibliography

[1] Rodney J. Baxter. *Exactly solved models in statistical mechanics*. Reprint of the 1982 original. Academic Press, Inc. [Harcourt Brace Jovanovich, Publishers], London, 1989, pp. xii+486. ISBN: 0-12-083182-1.

[2] Jérémie Bouttier, Guillaume Chapuy, and Sylvie Corteel. "From Aztec diamonds to pyramids: steep tilings". In: *Trans. Amer. Math. Soc.* 369.8 (2017), pp. 5921–5959. ISSN: 0002-9947. DOI: 10.1090/tran/7169.

[3] Alexey Bufetov and Alisa Knizel. "Asymptotics of random domino tilings of rectangular Aztec diamonds". In: *Ann. Inst. Henri Poincaré Probab. Stat.* 54.3 (2018), pp. 1250–1290. ISSN: 0246-0203. DOI: 10.1214/17-AIHP838.

[4] F. Colomo and A. G. Pronko. "The role of orthogonal polynomials in the six-vertex model and its combinatorial applications". In: *J. Phys. A* 39.28 (2006), pp. 9015–9033. ISSN: 0305-4470. DOI: 10.1088/0305-4470/39/28/S15.

[5] Louis Comtet. *Advanced combinatorics*. enlarged. The art of finite and infinite expansions. D. Reidel Publishing Co., Dordrecht, 1974, pp. xi+343. ISBN: 90-277-0441-4.

[6] Sylvie Corteel, Frederick Huang, and Christian Krattenthaler. "Domino tilings of generalized Aztec triangles". preprint. 2023.

[7] Sylvie Corteel and Jeremy Lovejoy. "Overpartitions". In: *Trans. Amer. Math. Soc.* 356.4 (2004), pp. 1623–1635. ISSN: 0002-9947. DOI: 10.1090/S0002-9947-03-03328-2.

[8] Philippe Di Francesco. "Twenty vertex model and domino tilings of the Aztec triangle". In: *Electron. J. Combin.* 28.4 (2021), Paper No. 4.38, 50. DOI: 10.37236/10227.

[9] Philippe Di Francesco and Emmanuel Guitter. "Twenty-vertex model with domain wall boundaries and domino tilings". In: *Electron. J. Combin.* 27.2 (2020), Paper No. 2.13, 63. DOI: 10.37236/8809.

[10] Noam Elkies et al. "Alternating-sign matrices and domino tilings. I". In: *J. Algebraic Combin.* 1.2 (1992), pp. 111–132. ISSN: 0925-9899. DOI: 10.1023/A:1022420103267.

[11] Ira Gessel and Gérard Viennot. "Binomial determinants, paths, and hook length formulae". In: *Adv. in Math.* 58.3 (1985), pp. 300–321. ISSN: 0001-8708. DOI: 10.1016/0001-8708(85)90121-5.

[12] A. M. Hamel. "Determinantal forms for symplectic and orthogonal Schur functions". In: *Canad. J. Math.* 49.2 (1997), pp. 263–282. ISSN: 0008-414X. DOI: 10.4153/CJM-1997-013-5.

[13] S. B. Kelland. "Twenty-vertex model on a triangular lattice". In: *Australian Journal of Physics* 27 (Dec. 1974), p. 813. DOI: 10.1071/PH740813.

[14] R. C. King. "Weight multiplicities for the classical groups". In: *Group theoretical methods in physics (Fourth Internat. Colloq., Nijmegen, 1975)*. Lecture Notes in Phys., Vol. 50. Springer, Berlin, 1976, pp. 490–499.

[15] C. Krattenthaler. "Identities for classical group characters of nearly rectangular shape". In: *J. Algebra* 209.1 (1998), pp. 1–64. ISSN: 0021-8693. DOI: 10.1006/jabr.1998.7531.

[16] Christian Krattenthaler. "A bijective proof of the hook-content formula for super Schur functions and a modified jeu de taquin". In: vol. 3. 2. The Foata Festschrift. 1996, Research Paper 14, approx. 24. DOI: 10.37236/1272.

[17] Greg Kuperberg. "Another proof of the alternating-sign matrix conjecture". In: *Internat. Math. Res. Notices* 3 (1996), pp. 139–150. ISSN: 1073-7928. DOI: 10.1155/S1073792896000128.

[18] Bernt Lindström. "On the vector representations of induced matroids". In: *Bull. London Math. Soc.* 5 (1973), pp. 85–90. ISSN: 0024-6093. DOI: 10.1112/blms/5.1.85.

[19] OEIS Foundation Inc. *The On-Line Encyclopedia of Integer Sequences*. Published electronically at http://oeis.org. 2023.

[20] Marko Petkovsek, Herbert Wilf, and Doron Zeilberger. *A=B*. A K Peters, 1996.

[21] James Propp and Richard Stanley. "Domino tilings with barriers". In: *J. Combin. Theory Ser. A* 87.2 (1999), pp. 347–356. ISSN: 0097-3165. DOI: 10.1006/jcta.1999.2967.

[22] Jessica Striker. "Poset and Polytope Persectives on Alternating Sign Matrices". PhD thesis. University of Minnesota, 2008.

[23] Doron Zeilberger. "Proof of the alternating sign matrix conjecture". In: vol. 3. 2. The Foata Festschrift. 1996, Research Paper 13, approx. 84. URL: http://www.combinatorics.org/Volume_3/Abstracts/v3i2r13.html.

Appendix A

Computations

Here we carry out a couple computations from Section 3.4.

Computation A.0.1.

$$\prod_{j=0}^{\lfloor \frac{k}{2} \rfloor} \prod_{i=-2k+4j-1}^{-k+2j-1} (2k+i+2) \cdot \prod_{j=0}^{\lfloor \frac{k-1}{2} \rfloor} \prod_{i=k-2j+1}^{2k-4j} (2k+i+2) \Bigg/ \prod_{j=1}^{k} (2j+1)^{k+1-j}$$
$$= \prod_{j=0}^{\lfloor \frac{k-1}{2} \rfloor} \prod_{i=-2k+4j+1}^{-k+2j} (2k+i+3) \cdot \prod_{j=0}^{\lfloor \frac{k-2}{2} \rfloor} \prod_{i=k-2j+2}^{2k-4j} (2k+i+3) \Bigg/ \prod_{j=1}^{k-1} (2j+1)^{k-j}$$

Proof. We This is an equality of two fractions; we bring both numerators to the left hand side and both denominators to the right hand side:

$$\frac{\prod_{j=0}^{\lfloor \frac{k}{2} \rfloor} \prod_{i=-2k+4j-1}^{-k+2j-1} (2k+i+2)}{\prod_{j=0}^{\lfloor \frac{k-1}{2} \rfloor} \prod_{i=-2k+4j+2}^{-k+2j+1} (2k+i+2)} \cdot \frac{\prod_{j=0}^{\lfloor \frac{k-1}{2} \rfloor} \prod_{i=k-2j+1}^{2k-4j} (2k+i+2)}{\prod_{j=0}^{\lfloor \frac{k-2}{2} \rfloor} \prod_{i=k-2j+1}^{2k-4j-1} (2k+i+2)} = \prod_{j=1}^{k} (2j+1)$$

When k is even this results in

$$(2k+1) \prod_{j=0}^{\frac{k}{2}-1} \frac{(4j+1)(4j+2)(4j+3)(4k-4j+2)}{(k+2j+3)(k+2j+2)} = \prod_{j=1}^{k} (2j+1)$$
$$\prod_{j=0}^{\frac{k}{2}-1} \frac{(4j+2)(4k-4j+2)}{(k+2j+3)(k+2j+2)} = 1$$

Similarly when k is odd we have

$$\frac{2k+4}{2k+4}\prod_{j=0}^{\frac{k-1}{2}}\frac{(4j+1)(4j+2)(4j+3)(4k-4j+2)}{(k+2j+3)(k+2j+2)}=\prod_{j=1}^{k}(2j+1)$$

$$\prod_{j=0}^{\frac{k-1}{2}}\frac{(4j+2)(4k-4j+2)}{(k+2j+3)(k+2j+2)}=1$$

We can verify that both of these identities do hold true. For even k the product on the left hand side expands as

$$\begin{aligned}\frac{2\cdot 6\cdots(2k-2)\cdot(2k+6)(2k+10)\cdots(4k+2)}{(k+2)(k+3)\cdots(2k+1)}&=\frac{2^{k/2}(k-1)!!2^{k/2}\frac{(2k+1)!!}{(k+1)!!}}{\frac{(2k+1)!}{(k+1)!}}\\&=\frac{2^k(k-1)!!(k+1)!}{(k+1)!!}\cdot\frac{(2k+1)!!}{(2k+1)!}\\&=2^k k!\cdot\frac{1}{(2k)!!}=1\end{aligned}$$

where $k!!$ is the product of all integers from 1 to k with the same parity as k. Similarly for odd k we have

$$\begin{aligned}\frac{2\cdot 6\cdots(2k)\cdot(2k+4)(2k+8)\cdots(4k+2)}{(k+2)(k+3)\cdots(2k+2)}&=\frac{2^{(k+1)/2}k!!2^{(k+1)/2}\frac{(2k+1)!!}{k!!}}{\frac{(2k+2)!}{(k+1)!}}\\&=2^{k+1}(k+1)!\cdot\frac{(2k+1)!!}{(2k+2)!}=1\end{aligned}$$ □

Computation A.0.2.

$$\frac{G(n+1)}{G(n)}=\frac{2^n(4n+2)!n!!}{(3n+2)!(3n)!!}$$

where

$$G(n)=\prod_{j\geq 0}\left(\prod_{i=4j+1}^{n+2j}i\prod_{i=3n-2j}^{4n-4j-2}i\right)\Bigg/\prod_{j=1}^{n-1}(2j+1)^{n-j}$$

Proof. To compute $\frac{G(n+1)}{G(n)}$ we first note that for even n we have

$$G(n)=\left(\prod_{j=0}^{\frac{n-2}{2}}\prod_{i=4j+1}^{n+2j}i\cdot\prod_{j=0}^{\frac{n-2}{2}}\prod_{i=3n-2j}^{4n-4j-2}i\right)\Bigg/\prod_{j=1}^{n-1}(2j+1)^{n-j}$$

and for odd n we have

$$G(n)=\left(\prod_{j=0}^{\frac{n-1}{2}}\prod_{i=4j+1}^{n+2j}i\cdot\prod_{j=0}^{\frac{n-3}{2}}\prod_{i=3n-2j}^{4n-4j-2}i\right)\Bigg/\prod_{j=1}^{n-1}(2j+1)^{n-j}$$

Then we will first compute $\frac{G(n+1)}{G(n)}$ for when n is odd:

$$\begin{aligned}
\frac{G(n+1)}{G(n)} &= \left(\frac{\prod_{j=0}^{\frac{n-1}{2}}\prod_{i=4j+1}^{n+2j+1} i \cdot \prod_{j=0}^{\frac{n-1}{2}}\prod_{i=3n-2j+3}^{4n-4j+2} i}{\prod_{j=0}^{\frac{n-1}{2}}\prod_{i=4j+1}^{n+2j} i \cdot \prod_{j=0}^{\frac{n-3}{2}}\prod_{i=3n-2j}^{4n-4j-2} i}\right) \Bigg/ \left(\frac{\prod_{j=0}^{n}(2j+1)^{n+1-j}}{\prod_{j=0}^{n-1}(2j+1)^{n-j}}\right) \\
&= \prod_{j=0}^{\frac{n-1}{2}}(n+2j+1) \cdot \frac{(2n+4)!}{(2n+3)!} \cdot \prod_{j=0}^{\frac{n-3}{2}} \frac{(4n-4j-1)\cdots(4n-4j+2)}{(3n-2j)\cdots(3n-2j+2)} \Bigg/ (2n+1)!! \\
&= \frac{(2n)!!}{(n-1)!!} \cdot \frac{(2n+4)!}{(2n+3)!} \cdot \frac{\frac{(4n+2)!}{(2n+4)!}}{\frac{(3n+2)!}{(2n+3)!} \cdot \frac{(3n)!!}{(2n+1)!!}} \cdot \frac{1}{(2n+1)!!} \\
&= \frac{2^n n!(4n+2)!}{(n-1)!!(3n+2)!(3n)!!} = \frac{2^n(4n+2)!n!!}{(3n+2)!(3n)!!}
\end{aligned}$$

On the other hand when n is even:

$$\begin{aligned}
\frac{G(n+1)}{G(n)} &= \left(\frac{\prod_{j=0}^{\frac{n}{2}}\prod_{i=4j+1}^{n+2j+1} i \cdot \prod_{j=0}^{\frac{n-2}{2}}\prod_{i=3n-2j+3}^{4n-4j+2} i}{\prod_{j=0}^{\frac{n-2}{2}}\prod_{i=4j+1}^{n+2j} i \cdot \prod_{j=0}^{\frac{n-2}{2}}\prod_{i=3n-2j}^{4n-4j-2} i}\right) \Bigg/ \left(\frac{\prod_{j=0}^{n}(2j+1)^{n+1-j}}{\prod_{j=0}^{n-1}(2j+1)^{n-j}}\right) \\
&= (2n+1) \cdot \prod_{j=0}^{\frac{n-2}{2}} \left((n+2j+1)\frac{(4n-4j-1)\cdots(4n-4j+2)}{(3n-2j)\cdots(3n-2j+2)}\right) \Bigg/ (2n+1)!! \\
&= (2n+1) \cdot \frac{(2n-1)!!}{(n-1)!!} \cdot \frac{\frac{(4n+2)!}{(2n+2)!}}{\frac{(3n+2)!}{(2n+2)!} \cdot \frac{(3n)!!}{(2n)!!}} \cdot \frac{1}{(2n+1)!!} \\
&= \frac{2^n(4n+2)!n!!}{(3n+2)!(3n)!!}
\end{aligned}$$

□